TIME-RESOLVED STUDIES OF LIGHT PROPAGATION IN TISSUE

Diploma paper
by
Roger Berg

Lund Reports on Atomic Physics, LRAP-106
Lund, October 1989

CONTENTS PAGE

CONTENTS PAGE

1. ABSTRACT

This paper describes experiments performed with a time-resolved technique to enhance the contrast in optical transillumination of tissue. The technique has applications in light scanning off female breasts with the purpose of detecting breast cancer.

As a light source a pico-second laser-system was used, emitting 9 ps pulses. The laser was scanned over a tissue phantom with a minimum optical path length of 26 mm. An object with a higher optical absorption than that of the phantom was placed in the middle of the phantom. The object thus simulates a tumour which often has higher absorption due to increased vascularity. The light that was emitted from the phantom is detected through a spatial window with time-resolution. Because of the high degree of scattering in the phantom a temporal dispersion curve was obtained for the photon arrival times. By scanning over the object and only detecting the light that arrives very early an image representing a shadow of the object could be created. Since the light that arrives early at the detector must have travelled more directly from the laser to the detector, the contrast can be enhanced compared with the contrast obtained if the total light intensity is detected, i.e. time-integrated light scanning.

With an object of 4 mm in diameter in the middle of the phantom the maximum contrast obtained with this time-resolved technique is almost 30 compared with 1.6 using the normal time-integrating light scanning technique. The contrast is defined as the maximum amount of light detected with no object in the phantom divided by the minimum amount of light detected when the object is placed between the incident laser beam and the detector.

2. INTRODUCTION AND THEORY

2.1 Introduction

Breast cancer is today one of the most common causes of early death among women. To succeed in the treatment of cancer the tumour has to be detected as early as possible. The first method for breast cancer detection was introduced by Max Cutler in 1929 (Ref. 1). He simply illuminated the breast with a torch and tried to see the shadows of the tumours on the opposite side. The method was not very efficient and since then many new techniques have been introduced with the purpose of detecting breast cancer. The most common method today is mammography which uses X-rays. X-rays are, however, a form of ionizing radiation with the potential risk of causing mutagenicity. With the rapid development in the fields of computers, lasers and theory for tissue optics, new methods involving visible light are becoming more and more interesting.

This paper is the result of experiments with a method involving time-resolved laser-spectroscopy to improve the contrast in visible light transillumination for breast cancer detection, i.e. light scanning.

2.2 Cancer

Cancer is the common name for a pathological condition in which unrestrained growth of abnormal cells takes place in one or more organs in the human body. The cell growth gives rise to a tumour. Benign tumours grow slowly and are surrounded by connective tissue and the only damage they can do is through the pressure they exert on the surrounding tissue. Malignant tumours grow uncontrollably and infiltrate the surrounding tissue, growing into blood- and lymphatic vessels and into the cavities of the body. Cancer cells can be transported with the blood and the lymph to other organs where they can produce new tumours (metastases).

Today breast cancer is the most common type of cancer among women. In Sweden (population 8.5 million) there are 4500 cases of breast cancer detected every year and approximately 100 women die every month due to breast cancer. Breast cancer is the most common cause of early death among women aged 40-54. The exact cause of the cancer is of course impossible to determine but some factors increase the risk of developing breast cancer, e.g. prior breast cancer, smoking, firs pregnancy after 30, late menopause or early menarche (Ref. 2).

2.3 The breast

The female breast consists of skin, fat, glandular tissue and connective tissue. There is a considerable periodic variation in the structure of the breast due to the female hormone cycle. Younger breasts are more dense and consist of more glandular tissue than older breasts which are fattier. For this reason it is much more difficult to detect a cancer tumour in a young woman than it is in an older one. The structure of the breast also changes during pregnancy and after lactation ceases.

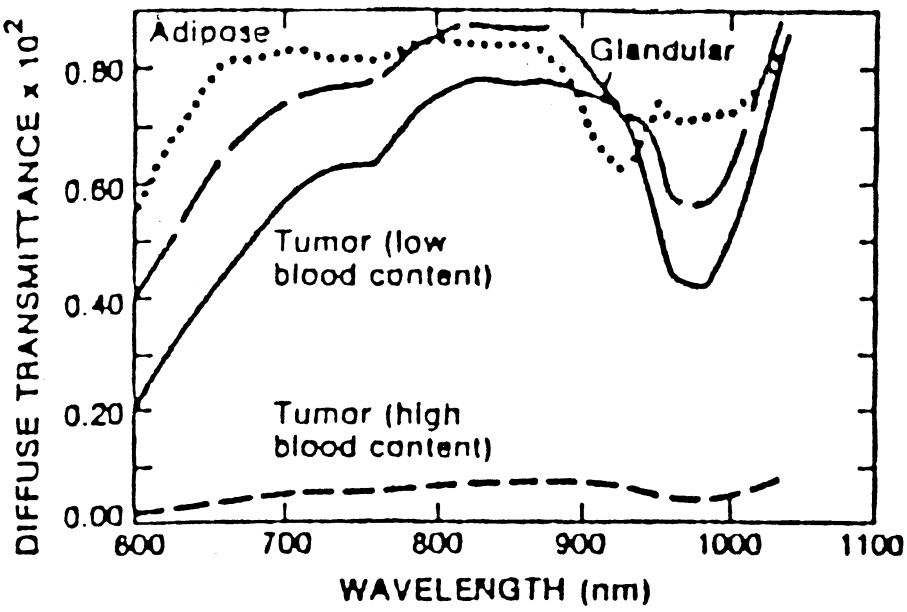

Fig. 1. *Diffuse transmittance versus wavelength for dissected breast tissue. Measurements were made within 8 h following the removal of tissue from body. From Ref. 3.*

A cancer tumour in the breast gives rise to a dense volume, often with increased concentration of blood vessels. The mean volume doubling time for the tumour is approximately 212 days, but with large variations (Ref. 2). A microcalcification in the breast is sometimes also an indication of a malignant tumour. Different methods of breast cancer detection attempt to detect vascularities and small microcalcifications in order to identify a breast tumour. The easiest method is of course self examination where the woman tries to feel the tumour with the fingers, but this is a very coarse method and only large tumours can be felt.

2.4 Treatment

The most important factor for successful treatment of the cancer is early tumour detection. If the tumour is in an early stage it can be treated by excisional biopsy in combination with radiation therapy, hormone therapy or chemotherapy. If the tumour has advanced the only method of treatment is often mastectomy (Ref. 2).

2.5 The optics of human tissue

Today most methods for the detection of breast cancer involve some kind of penetration of the tissue by electromagnetic waves. The depth of penetration depends very much on the wavelength that is used. X-rays, which have a very short wavelength (10^{-7} - 10^{-13} m), have a very good penetration capability. If visible light (≈ 400-700 nm) is used the penetration capability is strongly dependent on the wavelength. In Fig. 1 the diffuse transmittance for different kinds of tissue as a function of the wavelength is shown (Ref. 3). The diffuse transmittance was measured with an incident beam of near monochromatic light and detected with an integrating sphere on the opposite side of the sample. The higher the diffuse transmittance, the more light has passed through the

tissue. In Fig. 2 the same kind of measurement is shown with a normal human breast *in vivo* as sample (Ref. 3). The results show that suitable light for penetrating tissue is near-infrared light, i.e. ≈ 700-950 nm (Refs. 3, 4, 5 and 6).

When visible light enters the tissue it can be:

a) reflected
b) absorbed
c) scattered

Reflection occurs when light passes from one medium to another with different refractive indices (n). The reflection also depends on the polarization and the angle of the incident light. The reflectance (R) is the fraction of light that is reflected. When the light passes from one medium with refractive index n1 to another medium with refractive index n2 the reflectance is:

$$R_{\perp} = \left((n1\cos\theta 1 - n2\cos\theta 2) \,/\, (n1\cos\theta 1 + n2\cos\theta 2) \right)^2$$

$$R_{\parallel} = \left((n2\cos\theta 1 - n1\cos\theta 2) \,/\, (n1\cos\theta 2 + n2\cos\theta 1) \right)^2$$

$R_{\perp}$ is the reflectance of the light polarized perpendicularly to the incident plane and $R_{\parallel}$ is the reflectance for the light polarized parallel to the incident plane. $\theta 1$ is the angle of incidence and $\theta 2$ the angle of transmission. The refractive index for water (which is the main constituent of the human body) is 1.33 and for fat or concentrated protein approximately 1.55. These differences causes reflection not only at the boundary of the tissue (the skin) but also inside the tissue. If the light passes from air into tissue at normal incidence about 2-4 % of the light is reflected.

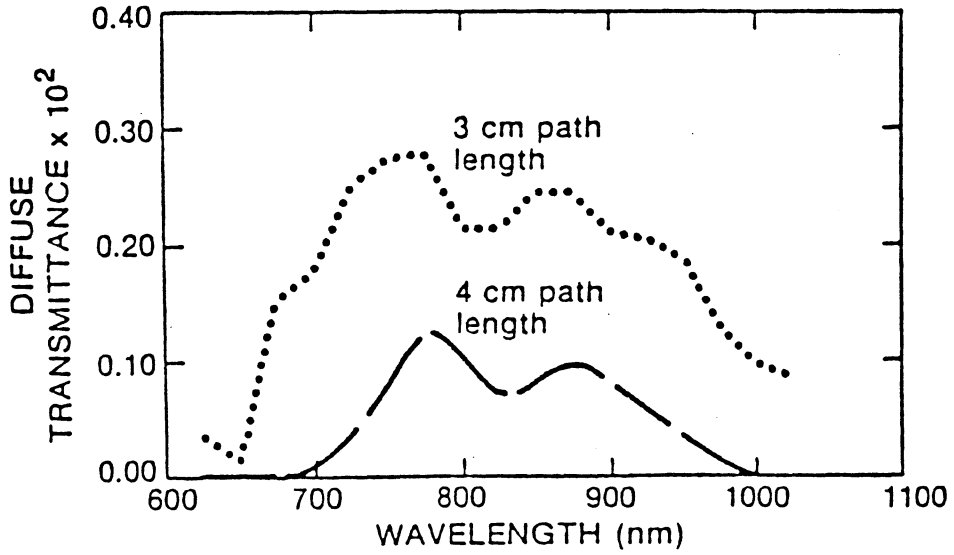

Fig. 2. In vivo *measurement of diffuse transmittance for intact nonmalignant human breast. From Ref. 3.*

The light that is not reflected enters the new medium and is thus transmitted into it. If there is no absorption or scattering at the boundary the transmission (T) is:

$$T_{\perp} = 1\text{-}R_{\perp}$$

$$T_{\parallel} = 1\text{-}R_{\parallel}$$

$T_{\perp}$ and $T_{\parallel}$ denote perpendicular and parallel polarization respectively as for the reflectance.

Absorption is described by the absorption coefficient β. In one dimension the formula is:

$$I(x) = I_o e^{-\alpha x}$$

Here I_o is the incident light intensity and I the intensity after a distance x. α is the effective attenuation coefficient which is the sum of β and a scattering coefficient. This formula assumes that the diffusion approximation is valid, i.e. at a considerable distance from the boundary (skin) where the light enters the tissue and thus the light distribution is almost isotropic. A useful concept is the penetration depth, which is defined as $\delta = 1/\alpha$.

Scattering occurs when a photon alters its path of flight due to collisions with matter. The electric field of the photon causes the electrons of the encountered atom or molecule to oscillate and the particle acts as a "light source" itself and can emit the photon in another direction. The scattered photon can have the same energy or a fraction of the energy it had before the collision. Scattering can be of different origins: Rayleigh scattering, Raman scattering or Mie scattering. Internal reflection, i.e. reflections inside the particle due to variations in the refractive indices, can also contribute to the scattering. The size of the particle is an important factor in determining the characteristics of the scattered light.

If the scattering particle is very small compared with the wavelength of the light Rayleigh and Raman scattering can occur. The scattered light is weak, polarized and almost isotropic. The scattering probability is proportional to $1/\lambda^4$ (λ=wavelength) and thus blue light is more likely to be scattered than red light (Rayleigh scattering makes the sky blue). Raman scattering is an inelastic form of scattering, i.e. the scattered photon has less energy than the incident photon.

Mie scattering is an elastic form of scattering and it occurs when the scattering particle is larger than the wavelength of the light. The relative cross section for Mie scattering is a complicated function of the wavelength, the particle radius, refractive indices and absorption. The intensity of the scattered light is approximately proportional to $1/\lambda^2$.

2.6 Mammography

Mammography is today the most common method used to detect breast cancer. The breast is compressed between two flat perspex plates to a thickness of about 2-3 cm. A photographic plate is placed behind the breast which is exposed to a soft X-ray source. The tumour is detected on the photographic plate as an area which has absorbed more of the X-ray radiation than the healthy tissue. To increase the probability of

detecting a tumour three exposures are often taken, one with the breast compressed horizontally, one vertically and one in between (45^{o}).

The problem in interpreting the X-ray plates is that the tumours and the healthy tissue can vary in structure and density. This sometimes makes it difficult to find even a large tumour in a dense breast, i.e. a breast with a lot of glandular tissue. On the other hand, tumours down to a size of 3-5 mm can be detected in less dense, i.e. fattier, breasts. The size of the breast is also an important factor. The more the breast can be compressed the easier it is to find a tumour. The interpreter has to develop some kind of intuition to find the tumours. Another problem is that tumours close to the body can be difficult to detect due to the round shape of the trunk.

To be able to detect breast cancer as early as possible it is desirable to perform mammography on as many women as possible (screening). This brings about a problem: X-rays constitue ionizing radiation and can induce cancer, even if as soft X-ray radiation as possible is used. The risk of undergoing mammography is of course difficult to estimate, but a risk analysis indicates that the benefit/risk ratio for asymptomatic women, aged 35-49 when the screening begins, is approx. 3.4 to 1 (worst case). For younger women the ratio is even less since younger women are probably more sensitive to ionizing radiation (Ref. 2).

Certain groups of women should be excluded from mammograpy, e.g. pregnant women, those who are undergoing post-surgical follow-ups, if they suffer from nipple discharge and of course those who do not wish to be examined by X-rays (Ref. 7). To improve the detection probability and to minimize the risk a great deal of effort is being devoted to finding new techniques not involving X-rays.

2.7 Thermography and ultrasonography

Thermography is a method which utilizes the heat produced in a tumour for its detection. All tumours have increased metabolism and this makes them warmer than the surrounding tissue. Liquid crystals or infrared detectors can be used to detect the heat.

Since the tumour is often more dense than the surrounding tissue it is sometimes possible to detect it by ultrasonography. A sound wave is sent into the breast by a transducer. The tumour will give rise to an echo due to a change in the acoustic impedance. The echo is detected by the transducer and the result can be analysed and displayed on a monitor (Ref. 2).

2.8 Methods using visible light

The first attempt to perform transillumination of the breast for the purpose of detecting breast cancer, was, as previously mentioned, by Max Cutler in 1929. The result was rather disappointing since he could not distinguish tumours from other normal noncystic structures in the breast. With the development of new equipment the idea of using visible light for screening has been reintroduced. It has developed into methods called light scanning and diaphanography. The idea is to transilluminate the breast with some kind of light source. Since tumours have a different absorption coefficient from the healthy tissue a "shadow" of the tumour is created on the opposite side of the breast and by detecting

this decrease in light intensity the cancer can be identified. The size, structure and location (with respect to the skin) of the tumour are of significant importance in the probability of detecting it (Ref. 8). A tumour close to the skin is much easier to detect than a tumour in the middle of the breast.

Diaphanography is a method in which a photographic film is used as a detector, and was introduced by Gros, Quenneville and Hummel in 1972. They used a very intense light source and discovered that light with longer wavelengths was more suitable for the transillumination of tissue (Ref. 9).

Ohlsson et al. developed this method by using infrared film to increase the contrast. They managed to detect 10 out of 11 malignant tumours among 107 patients with this method (Ref. 9).

Another method employs a video camera as a detector. This makes it possible to digitize the image and analyse it in a computer. Carlsen uses a technique where the breast is illuminated by light of two different wavelengths and the transmitted light is detected with a video camera (Ref. 7). The two images obtained at with the two wavelengths are digitized and by using an algorithm in which the luminance and the transmission ratio are calculated a colour image showing areas with unusual absorption can be obtained. These areas are possible tumours.

Today light scanning equipment is produced and sold commercially but to improve the results greater effort has to be made to educate and train the interpreter (the physician) since the results are not always easily evaluated.

2.9 Tomographic methods

To enhance the contrast and to create a three-dimensional image when X-rays, ultra sound or visible light are used, a tomographic method can be utilized. In this technique the object is scanned from different angles, in slices, and thus several images are obtained. The images are digitized and a computer can then use a mathematical algorithm to create a three-dimensional image of the object.

To detect breast cancer the tomographic method can be used when performing light scanning. The breast is scanned with visible light and the detected light is digitized and manipulated by a computer. In this way the contrast can be enhanced. Some experiments have been performed on breast phantoms with satisfactory results (Refs. 2, 10 and 11).

2.10 Time-resolved spectroscopy

The dominating effects when light passes through tissue are absorption and scattering. When performing time-resolved spectroscopy the scattering effect is very obvious. Due to multiple scattering in the tissue a considerable temporal dispersion of a short incident light pulse will occur. The width of the dispersion curve is also affected by the absorption in the tissue. The more absorption the less the temporal dispersion. This effect can be used to monitor blood and tissue oxygenation, especially in the brain (Ref. 12). The less oxygenation the higher the absorption coefficient and thus the light decays faster in the temporal dispersion curve, see Fig. 3. This figure shows the result

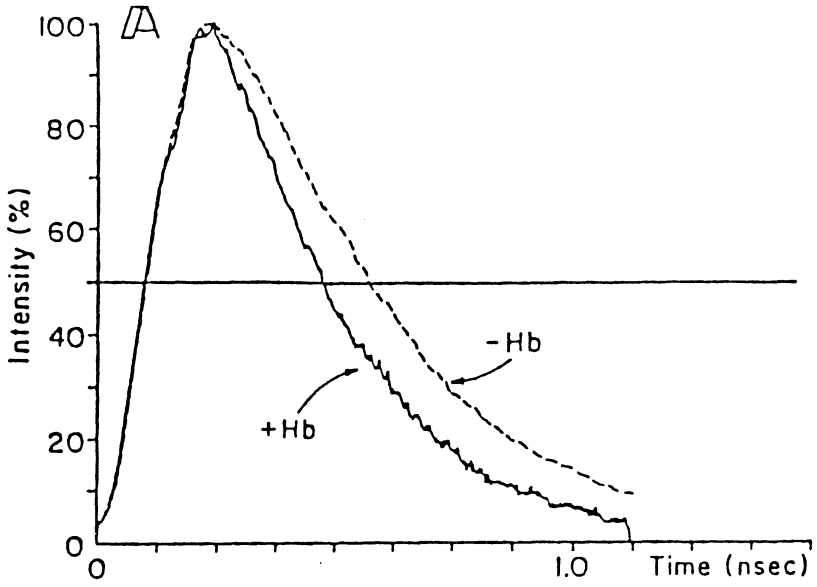

Fig. 3. *The effect of the presence of haemoglobin in a cat head model. Pulsed light measurements at 760 nm. With (+Hb) and without (-Hb) haemoglobin. From Ref. 13.*

when 10 ps laser pulses enter a model simulating the head and brain of a cat and the output light is monitored perpendicularly to the incident light (Ref. 13). The curve labelled -Hb is the result when no haemoglobin is present and +Hb is when haemoglobin has been injected into the model. As can be seen the dispersion decreases in the presence of haemoglobin which is highly absorbing at the wavelength used.

Delpy et al. have estimated the optical path length in tissue (Ref. 14). In Fig. 4 the temporal dispersion curves for the light passing through a rat head are displayed. The different curves are for different degrees of oxygenation of the blood, i.e. the rat has inhaled gases with different concentrations of oxygen. The results show that when 5 % of the total intensity has been detected a time corresponding to a distance of 2.5 times the diameter of the rat head has passed since the light first struck the head. Correspondingly, when 50 % of the total intensity has been detected the light has travelled 4.9 times the diameter of the rat head and for 95 % of the light the equivalent figure is 9.4 times the rat head. These results correspond to a refractive index of 1.4 when the rat had inhaled gas with 21 % O_2. The mean distance across the rat head was 1.46 cm.

The curves show a considerable temporal dispersion and this is due to a strong multiple scattering effect.

To simulate the propagation of light through tissue a Monte Carlo model can be used. This is a computer model where the photons enter the tissue one by one and perform some kind of "random walk" in the tissue. The parameters that determine the photon propagation are the absorption coefficient, the scattering coefficient and the phase function, i.e. the angular distribution of the scattered light. By detecting the photons that exit the tissue through e.g. a spatial window versus the elapsed time a temporal dispersion curve can be obtained.

The model shows good agreement with the results obtained experimentally (Refs. 14, 15, 16 and 17).

2.11 The purpose of this project

Multiple scattering in tissue is also observable in transillumination. An obvious example is to transilluminate the hand with a torch. It is easy to observe the transmitted light but no shadows of the bones are seen due to multiple scattering. When transillumination of female breast is carried out this effect is very obvious and lowers the contrast between the healthy tissue and the tumour.

This project is focused on a method involving time-resolved laser spectroscopy to enhance the contrast in the light scanning images. The idea is to use a laser with very short pulses, i.e. a pico-second laser, as a

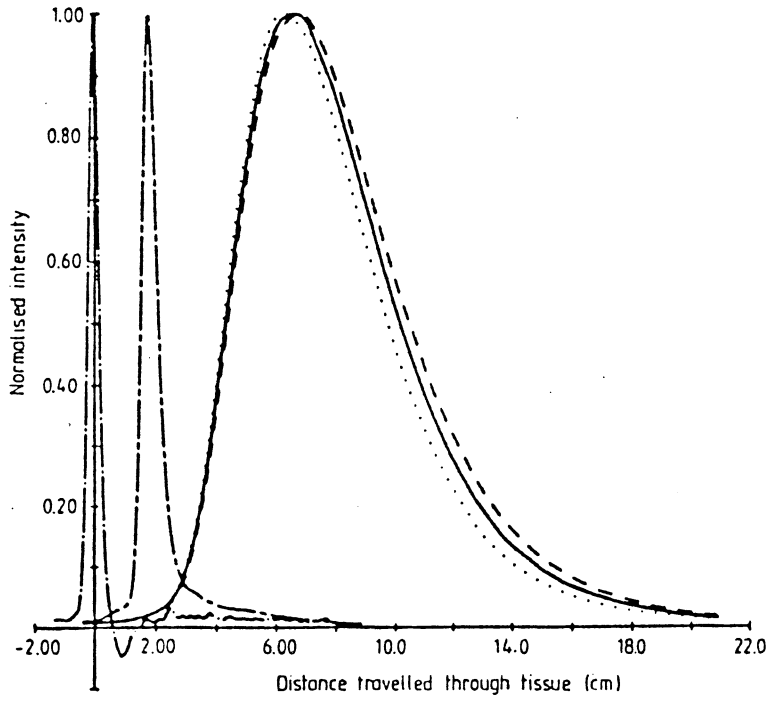

Fig. 4. *Measurements in vivo across a rat head (n = 1.4) at 783 nm.The input pulse (—— • ——) is at the origin and coincides with light first entering the head. The different profiles are obtained when the rat inhales different mixtures of gases. 100% O2 (— — —), 21% O2 (———), 12% O2 (• • • • •), balanced with N2. The decrease in cerebral oxygenation produces an increase in absorption in the brain tissue. The remaining profile (—— - ——) shows the result with the brain removed and the skull filled with silicon oil (n = 1.4). From Ref. 14.*

light source. The pulses hit a tissue phantom with high scattering quality. On the opposite side of the phantom an optical system detects the transmitted light. The data are evaluated so that an intensity-time curve is obtained, i.e. a temporal dispersion curve. A solid object is introduced into the phantom. This object simulates a cancer tumour as it has a higher absorption coefficient than the phantom. The goal is to locate this object. The object is located in the middle of the scattering phantom where it is most difficult to find it by means of ordinary methods.

If the object is located between the incident light beam and the detector some of the light will be absorbed. But the light that reaches the detector early, i.e. the light on the positive slope of the time dispersion curve, ought to be more absorbed than the rest of the light because the early light has travelled in a straighter path to the detector. By scanning over the object, i.e. measuring at different points in the object, and gating only on the early light, a curve representing some kind of shadow of the object can be created and thus the object can be detected.

3. METHODS AND MATERIALS

3.1 The pico-second laser system

In Fig. 5 the experimental arrangement for time-resolved light scanning is shown. As a light source a pico-second laser system is used, which consists of a mode-locked Coherent CR-3000K Ar^+ laser pumping a Coherent CR-599 dye laser with a Coherent 7210 cavity dumper.

The Ar^+ laser works at a wavelength of 514 nm and it has a mode-locker head attached. The mode-locker head is a prism placed in front of one of the cavity mirrors. The prism is modulated by a radio frequency (RF) source. The RF source creates an acoustic standing wave in the prism and this induces losses in the cavity in a loss cycle corresponding to the round trip time for one pulse in the cavity, i.e. the round trip time = 2L/c where L=the cavity length and c=the speed of light. The output pulsewidth from the Ar^+ laser is approximately 100 ps (FWHM) and the output pulse rate is 75 MHz. The average output power is approximately 1 W.

The Ar^+ laser pumps a dye laser which has DCM as the active medium. The dye laser is mode-locked by synchronous pumping, i.e. the cavity lengths of the Ar^+ laser and the dye laser are the same. This is achieved by introducing a delay-line into the dye laser. The Ar^+ laser thus only pumps one pulse in the dye laser. To obtain an output pulse from the dye laser a cavity dumper is used.

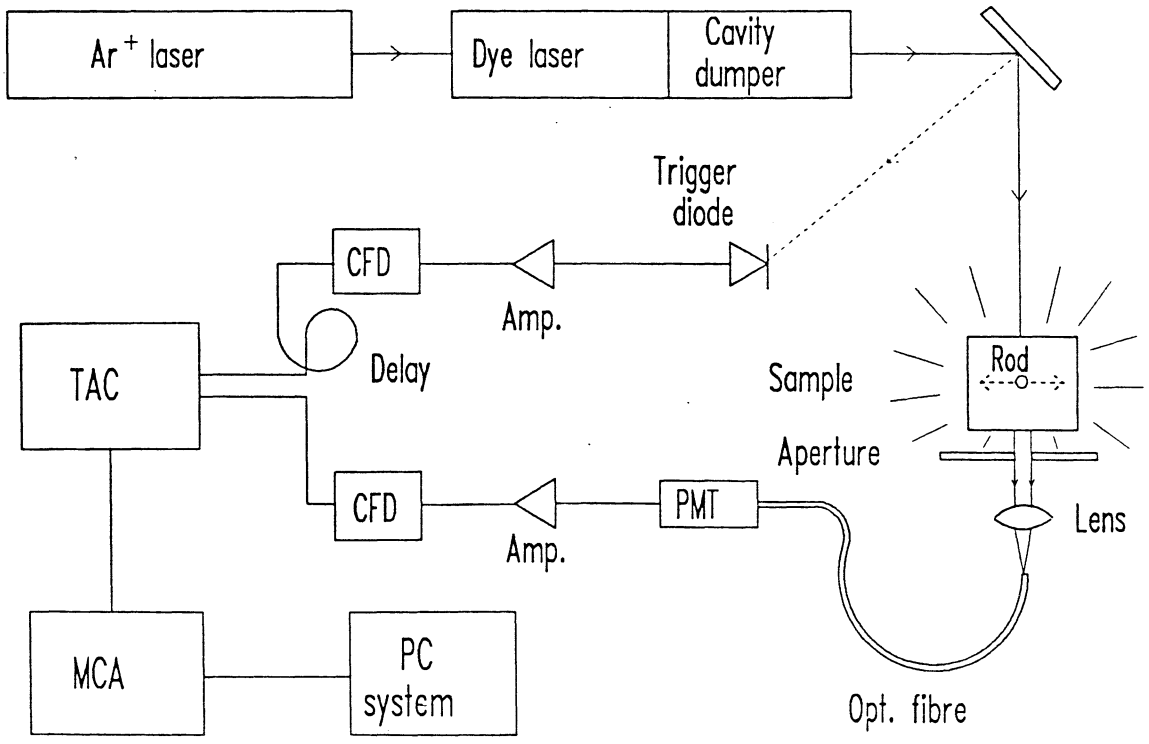

Fig. 5. *The experimental set-up.*

The dumper consists of two highly reflecting mirrors with a Bragg cell in between. A Bragg cell is an acousto-optic modulator in which all the diffracted light is of the first order. The cell is modulated with a 380 MHz RF signal. The pulse repetition frequency can be chosen by sending the modulation signal in pulses that are shorter than the round trip time and separated by a multiple of the round trip time. The repetition frequency is f_0/N where f_0 is the frequency used in the Ar^+ laser mode-locker head and N is an integer that can be chosen arbitrarily. Large values of N give a low repetition frequency but the output peak power will be larger since the pulse is amplified more before it is released by the cavity dumper. The cavity dumper is synchronized with the mode-locker head.

The output pulse from the dye laser is approximately 9 ps (FWHM) and the average output power is 50 mW in CW mode which means that the Bragg cell is modulated constantly which gives a pulse from the dye laser for every pulse from the Ar^+ laser. The dye laser is tuned to a wavelength of approximately 665 nm, i.e. in the red region. The wavelength is not very critical in this experiment since the tissue phantom is white and the extinction is not very wavelength dependent.

3.2 The autocorrelator

The pulse width is measured with an autocorrelator constructed at the Department of Physics, Lund Institute of Technology, Lund (Ref. 18). The autocorrelator measures the pulse width by dividing it into two beams with a beam splitter. One of the beams is delayed by means of a movable prism and the two beams are focused together under certain angular conditions in a KDP crystal causing frequency doubling to occur.

By measuring the intensity of the frequency-doubled light with a photomultiplier and displaying the signal as a function of the position of the movable prism on an XY oscilloscope the pulse width can be determined. Since the displayed pulse is proportional to the autocorrelation of the pulse and the pulse can be considered to have a Gaussian shape the FWHM of the displayed pulse is $\sqrt{2}$ times larger than the FWHM of the incident pulse.

For further information about the laser system and the autocorrelator see Appendices A and B.

3.3 The detection technique

The time-resolved detection technique used in this experiment is a photon counting method called delayed coincidence-technique. The method uses a detector signal and a trigger signal. The detector signal is induced by one photon only and thus the detector signal and the trigger signal will be separated by a different time interval depending on the delay of the photon, i.e. where on the time dispersion curve it belongs. A converter measures the time difference between the two signals and a count is added to a channel, corresponding to the time difference, in a multichannel analyser. Thus a time vs. intensity curve is built up in the multichannel analyser. Since one detected photon corresponds to one incident laser pulse the repetition frequency of the laser has to be rather high.

The method implies that the probability to obtain a signal from the detector is much less than one for every laser pulse that reaches the

sample. Otherwise, if more than one photon reached the detector during a triggering sequence only the first photon would be detected and the result would be false. This effect is called pile-up.

It should be noted that the experimental set-up used in this project uses the detector signal as the start signal and the trigger signal as the stop signal in order to reduce the system dead-time.

3.4 The detector

On the detector side the light passes through a 1 mm wide aperture. Approximately 30 mm behind the aperture there is a 3 mm diameter lens with a focal length of 4 mm. The lens focuses the light onto the end of an optical fibre. The fibre is of silicone and has a core diameter of 600 μm and plastic cladding. The aperture, lens and fibre are mounted as one easily movable unit and the acceptance angle of the unit is approximately 2.9^{o}, i.e. the incident light must not have an angle larger than 1.45^{o} from the optical axis to be able to enter the detector. The length of the fibre is 1 m and the transmitted light is focused by a lens into the opening of a Hamamatsu 1564U-07 microchannel plate detector (MCP). The MCP is connected via a very short cable ($\approx$ 20 cm) to an EG&G-ESN VT110 fast amplifier. The amplifier signal is then fed to a Tennelec TC455 constant fraction discriminator (CFD).

The CFD is used to minimize the time ripple. It provides a logic output signal when the input signal has reached a fixed fraction of its maximum. This is done by splitting the signal into two parts and delaying one part by a short cable (a few cm long). The maximum value of the undelayed signal is measured. When the delayed signal reaches a fixed fraction of the maximum of the first signal the logical output signal is set. In this way a trigger signal is obtained that is more precise in time compared with the signal itself, independent of the amplitude of the signal, and thus the time ripple is minimized.

The output signal from the CFD is led to a Canberra 1443A time to amplitude converter (TAC). The TAC gives an output voltage that is proportional to the time difference between accepted logical start and stop inputs. The TAC is operated in the 100 nanosecond time range, which means that the maximum output voltage (10 V) is reached 100 ns after the TAC has been triggered at the start input. The signal from the MCP is connected to the start input on the TAC. The stop signal to the TAC comes from a fast photo-diode triggered by a reflex from the laser. The diode is connected to a VT110 fast amplifier through another channel of the CFD and through a 18 m long cable, which functions as a delay, to the stop input of the TAC. See Fig. 5. The delay cable causes the signal from the diode to arrive at the TAC after the signal from the MCP and thus a voltage proportional to the time elapsed between the start signal from the MCP and the stop signal from the diode is induced as output from the TAC.

The output signal from the TAC is connected to a Tracor Northern TN-1710 multichannel analyser (MCA). The MCA is operated in the 4096 channel mode which means that the maximum input voltage is split up between 4096 channels. When the MCA receives an input signal the channel corresponding to that voltage is increased by one. By sampling during a time set on the MCA a time dispersion curve is obtained. The dispersion curve is displayed on a monitor.

All in all, this detection system with these settings gives a resolution of approximately 20 ps per channel on the MCA. This value has been obtained in previous experiments with this equipment.

To avoid pile-up, not more than one photon is allowed to enter the MCP for every pulse from it. To get an idea of the risk of pile-up the counting rates, i.e. pulses/second, from the MCP as well as the diode must be detected. This was carried out with an Ortec Photon Counter connected to the TAC. The count rate from the MCP depends on the amount of light entering the detector and how well the light is focused into the MCP. The count rate from the diode should be the same as the pulse rate frequency from the laser but it is limited by the electronics and the diode itself since their responses are not fast enough.

3.5 Data analysis

The MCA is connected to a PC-compatible computer system. A multi-purpose program written in FORTRAN is used for data analysis. The program can read 1024 channels from the MCA. The channels read by the computer are selectable. The dispersion curves are stored on a hard disk as data files. The program can also display the curves on the computer monitor, perform mathematical operations on the curves and calculate the sum of a number of channels, etc. It is also possible to do Fourier transformations on the curves and to analyse up to five curves at the same time with the program.

The curves can be plotted on a laser printer.

The computer program is listed in Appendix C.

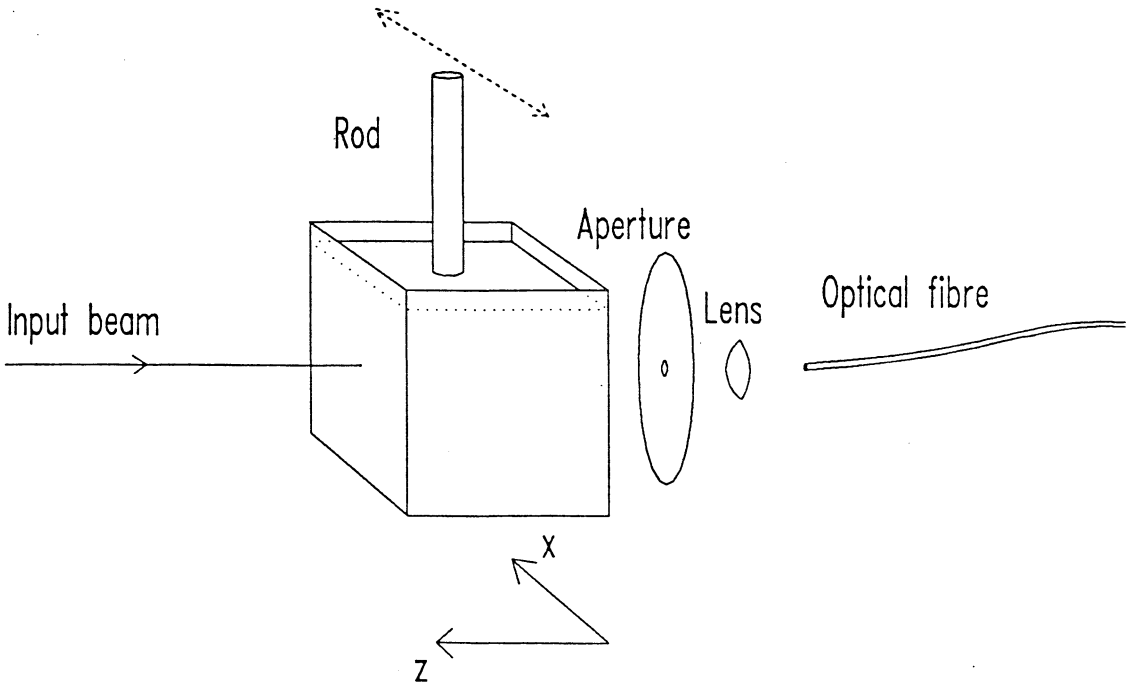

Fig. 6. *The sample and the optical part of the detector.*

3.6 The sample

The sample is supposed to simulate tissue, i.e. it should have good scattering characteristics. It must also be possible to introduce some sort of tumour phantom into it and the sample must be movable in some way to make scanning possible.

The sample, in most cases, consisted of a glass cuvette containing a scattering liquid inside. The inner dimensions of the cuvette were 26 mm wide, 25 mm high and 26 mm deep. This means that the scanning light has a minimum distance of 26 mm to travel through the sample. The scattering liquid is a liquid called "Polyclense", originally intended for cleaning contact lenses. The liquid is white and milky and consists of small plastic particles in a water solution. It is homogeneous and it does not stratify significantly with time. Figure 6 shows the arrangement of the sample and the optical part of the detector.

The tumour phantom used was a solid metal rod or thin plate. It is attached to a holder that is movable by means of a micrometer screw. In this way the object can be translated in the liquid and thus the scanning can be performed without moving the glass cuvette or the laser-detector system.

Other samples used were a hand *in vivo* and a piece of pork.

4 RESULTS

4.1 Time-integrated light scanning

The first question is, how difficult is it to detect the tumour object in the tissue phantom by looking at the light intensity. The phantom is the glass cuvette containing Polyclense and the object is a 4 mm diameter metal rod. In Fig. 7 the decrease in light intensity versus the position in the z direction of the rod. The decrease in the detected light intensity is evaluated as the light intensity with the object between the incident light beam and the detector divided by the light intensity detected without the object in the liquid. The z position of the rod is measured in mm from the wall closest to the detector (the coordinates are defined in Fig. 6). The dotted lines indicate the position of the walls of the phantom, i.e. a position of 13 mm means that the rod is in the middle of the cuvette. Not surprisingly, the contrast is lowest when the object is in the middle of the phantom, i.e. the object is most difficult to detect there.

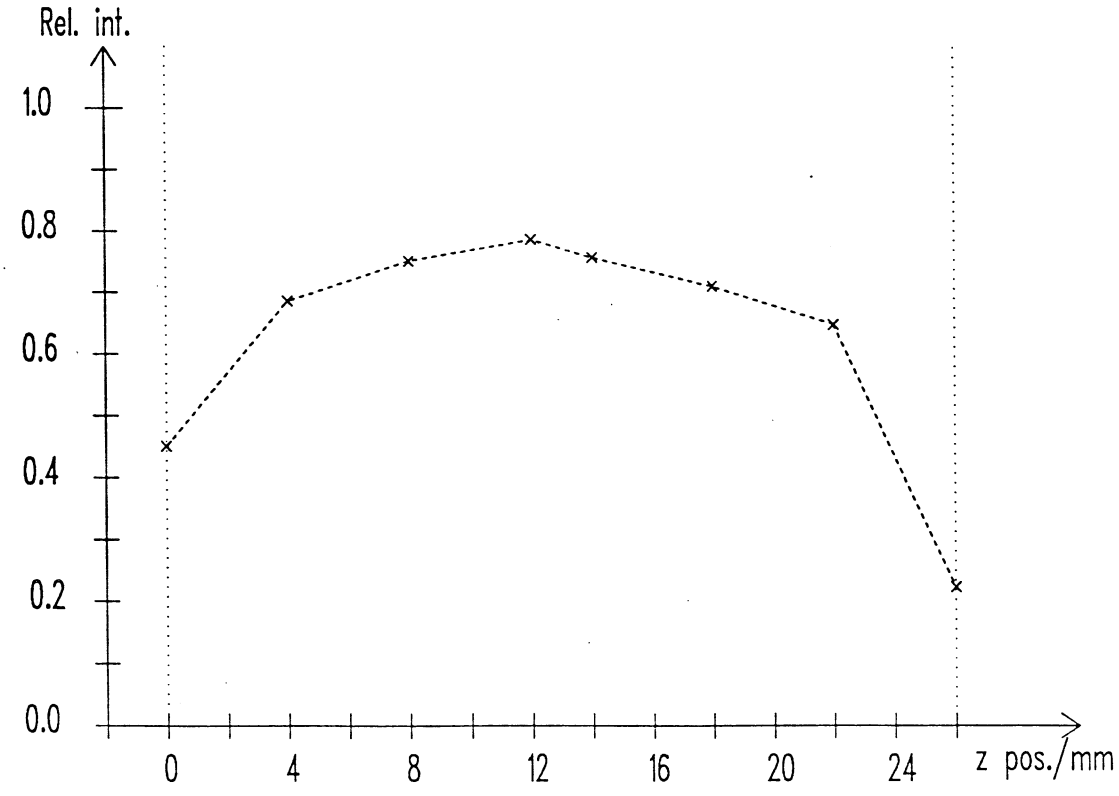

Fig. 7. *The relative light intensity (min. amount of light detected with the rod between the laser and the detector divided by the maximum amount of light detected without the rod in the liquid) versus the z position of the 4 mm rod. 0 mm denotes that the rod is as close as possible to the wall nearest the detector. The dotted lines indicate the walls of the phantom.*

4.2 Time-resolved detection

Without any phantom at all the pico-second laser and the time-resolved detection give a time dispersion curve as shown in Fig. 8. This curve is the apparatus function (or impulse response function) and is the result when the laser light is detected directly. Each dot represents one channel in the MCA which is approximately 20 ps in time. On the horizontal axis there is a mark every 50th channel, i.e. ≈ 1 ns. The FWHM of the curve is approx. 75 ps. This is the practical resolution of the detection system. The dispersion of the 9 ps incident pulses to this width is due to fluctuations and time ripple, mainly in the MCP.

When the glass cuvette with the scattering liquid is introduced the dispersion curves becomes much wider, as shown in Fig. 9. The sampling time is 120 seconds and the count rate from the MCP is 2600 counts per second (cps).

The noise during the sampling, i.e. the count rate without the incident laser beam, is 35 cps. The count rate from the trigger diode is approx. 250,000 cps. This means that the probability of pile-up is approx. 0.01 % ($\approx (2600/250{,}000)^2$).

Is this phantom a good substitute for tissue? Evidently the scattering properties of the liquid are very good. Five percent of the total light intensity is detected within a time corresponding to the time taken for the light to travel a distance of 3.0 times the length of the phantom. For 50 % of the total light intensity the figure is 7.8 times and for 90 % it is 13.3. All these figures are calculated with a refractive index of 1.33 for the liquid and thus the time taken for the light to travel across the phantom takes 115 ps, corresponding to 5.8 channels. The figures should be compared with the rat head results presented by Delpy et al. (Ref. 14) presented in Chapter 2.10. The results indicate that the scattering properties of the phantom are similar to those for living tissue.

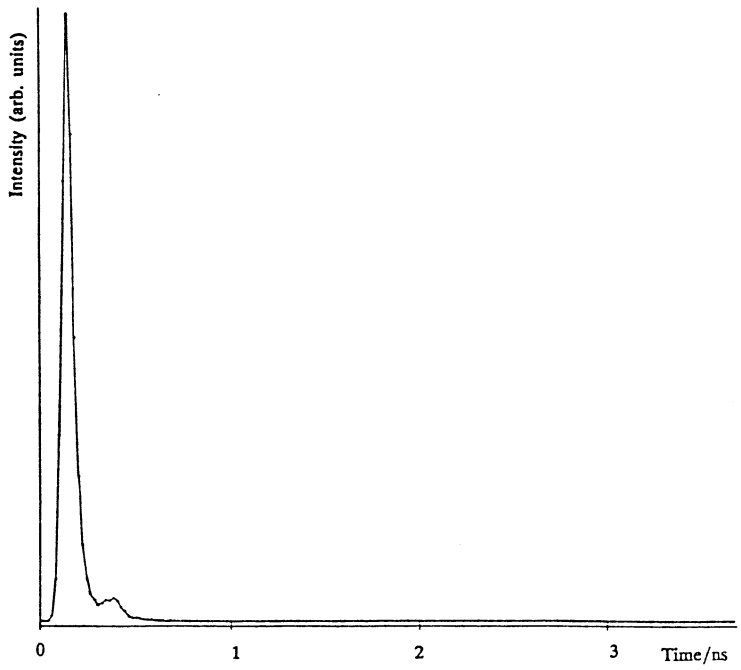

Fig. 8. *The apparatus function. Intensity (arbitrary units) versus time.*

Fig. 10 shows the dispersion curve for a human hand used as a sample. The region used was the soft part between the thumb and the index finger and it had a thickness of approximately 25 mm. The curve is somewhat noisier than that for the previous sample since the sampling time was only 60 s due to practical problems. The curve shows a dispersion of the same magnitude as the liquid phantom. Fifty percent of the total light intensity was received within a time corresponding to the time taken for the light to travel a distance of 7.0 times the thickness of the hand. This was calculated with a refractive index of 1.4.

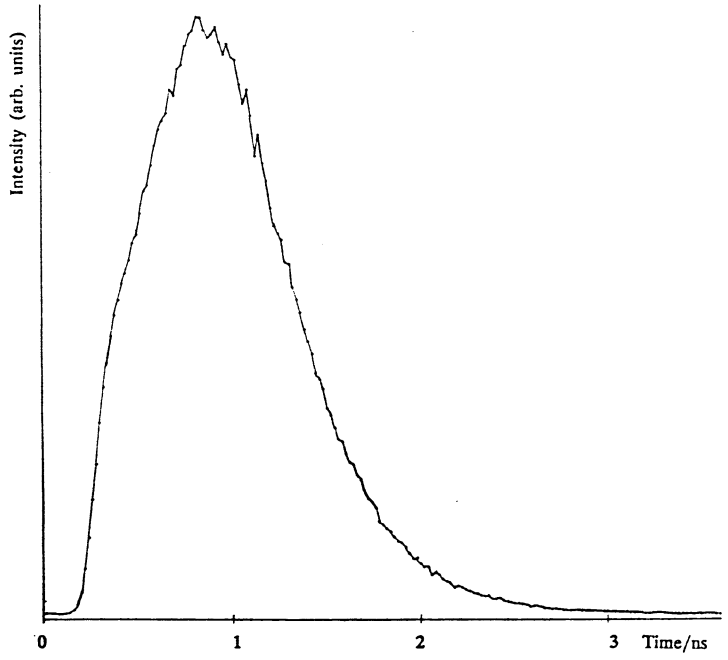

Fig. 9. *A temporal dispersion curve obtained with the tissue phantom.*

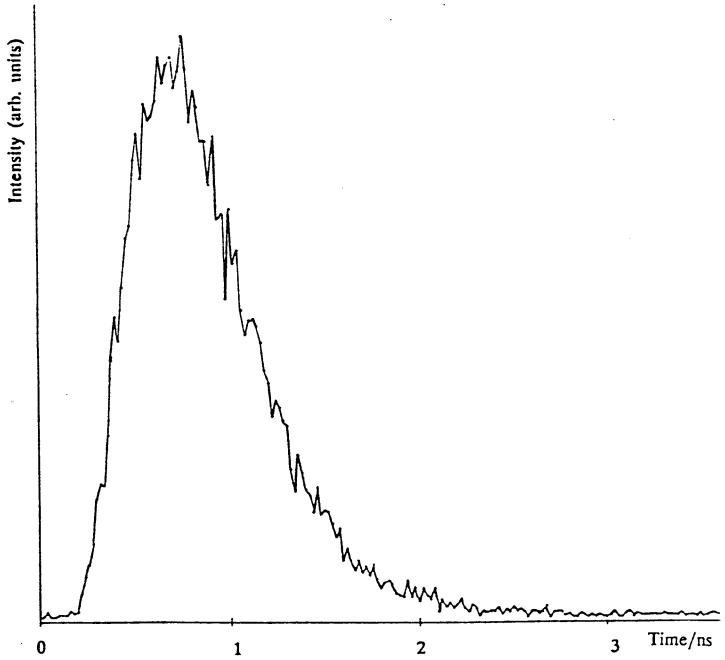

Fig. 10. *A dispersion curve obtained through the soft part of the hand between the index finger and the thumb (25 mm thick) in vivo.*

4.3 Deconvolution

The first step in evaluating the curves is to deconvolute the spread in the apparatus function from the recorded curves. This is a mathematical process to remove the influence of the dispersion of the apparatus function. The ideal form of the apparatus function is a delta function and by deconvoluting the received apparatus function with the sampled time dispersion curve the curve corresponding to an ideal apparatus function is obtained. If g(t) represents the apparatus function and f(t) the "true" curve, which we wish to find, the convolution of the two functions is h(τ), which is the curve we record. The convolution is:

$$h(\tau) = \int_{-\infty}^{\infty} g(t)f(t-\tau)\, d\tau$$

a.

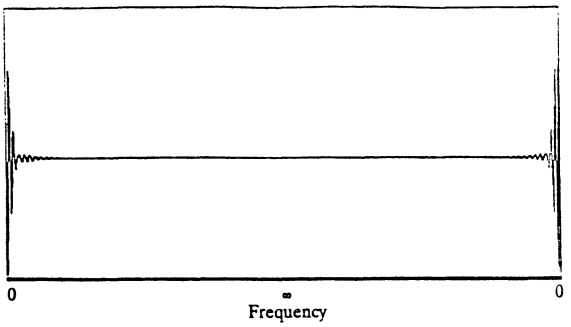

b.

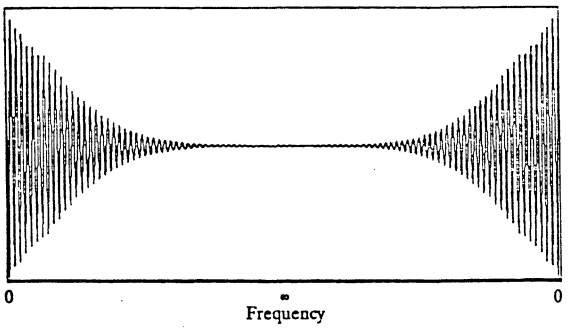

c.

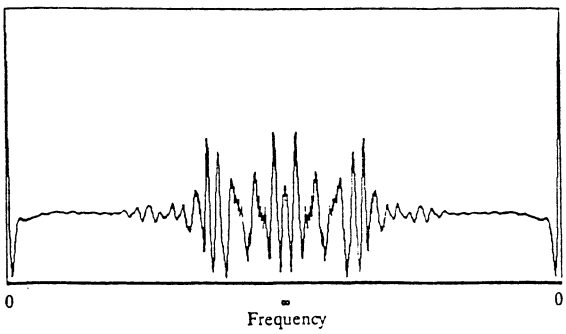

Fig. 11. *In figure* **a** *the real part of a Fourier transform of a typical dispersion curve is shown. The curve is symmetric about the centre with min. frequency at the ends of the curve and max. frequency in the centre. In figure* **b** *the real part of the Fourier transform of the apparatus function is shown. Figure* **c** *is the result when the transform in figure* **a** *is divided by the transform in figure* **b**.

This equation can be solved by means of Fourier transforms. If $\mathbb{F}(\ )$ denotes the Fourier transform and $\mathbb{F}^{-1}(\ )$ denotes the inverse Fourier transform then: $G(\omega)=\mathbb{F}(g(t))$, $F(\omega)=\mathbb{F}(f(t))$ and $H(\omega)=\mathbb{F}(h(t))$.
The convolution theorem states:

$$\mathbb{F}\left(\int_{-\infty}^{\infty} g(t)f(t-\tau)\, d\tau \right) = G(\omega)\cdot F(\omega)$$

$$\Leftrightarrow$$

$$G(\omega)\cdot F(\omega) = H(\omega)$$

And thus the required function f(t) is:

$$f(t) = \mathbb{F}^{-1}(H(\omega)/G(\omega))$$

The Fourier transformations (and inverse transformations) are performed in a Fast Fourier Transformation (FFT) computer subroutine. The subroutine is listed in Appendix C. The routine calculates a 512 channel complex Fourier transform. The real part of the Fourier transform of the apparatus function is displayed in Fig. 11b. The curve is symmetric about the centre and the lowest frequencies are at the ends of the curve and the highest in the centre. Fig. 11a shows the real part of the transform of a dispersion curve and Fig. 11c shows the result of dividing curve a by curve b. The inverse transformation of this curve is displayed in Fig. 12. As can be seen the result is very noisy. This is due to high frequencies that appear when the curve is deconvoluted.

Since the apparatus function is 75 ps the maximum frequency the system can respond to is $1/(75\cdot 10^{-12}) \approx 14$ GHz. Frequencies higher than this

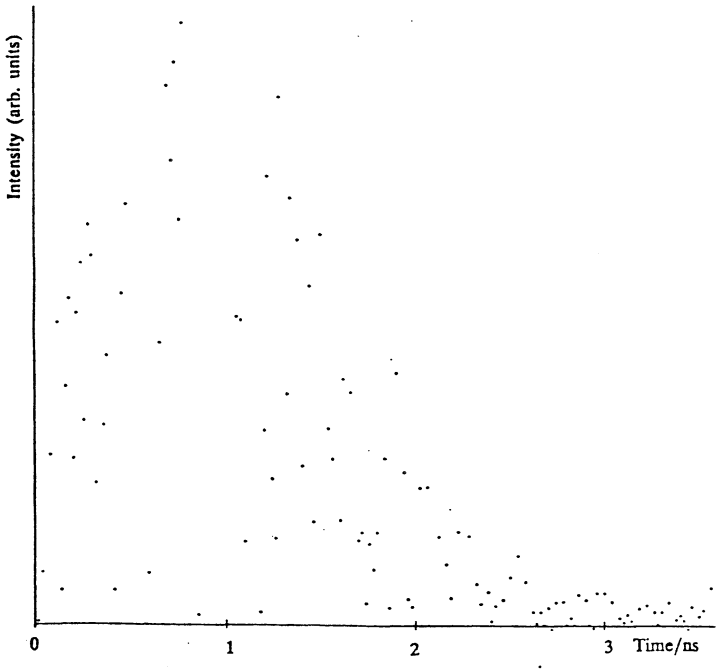

Fig. 12. *The result when the Fourier transform in Fig. 11c is inversely transformed.*

are not relevant and can thus be filtered away from the Fourier transforms. By creating a curve that is a sine wave with a period of 4 channels, which corresponds to 80 ps, and Fourier transforming it, it is possible to determine which channels in the Fourier transform are irrelevant. Fig. 13b shows the transform of the sine wave. By setting all channels between the two peaks to zero the Fourier transform can be filtered. This corresponds to channels 250 to 774. If the previously mentioned division between the two Fourier transforms (Fig. 13a) is filtered the result will be as shown in Fig. 13c. The result of the inverse transformation of this curve is displayed in Fig. 14.

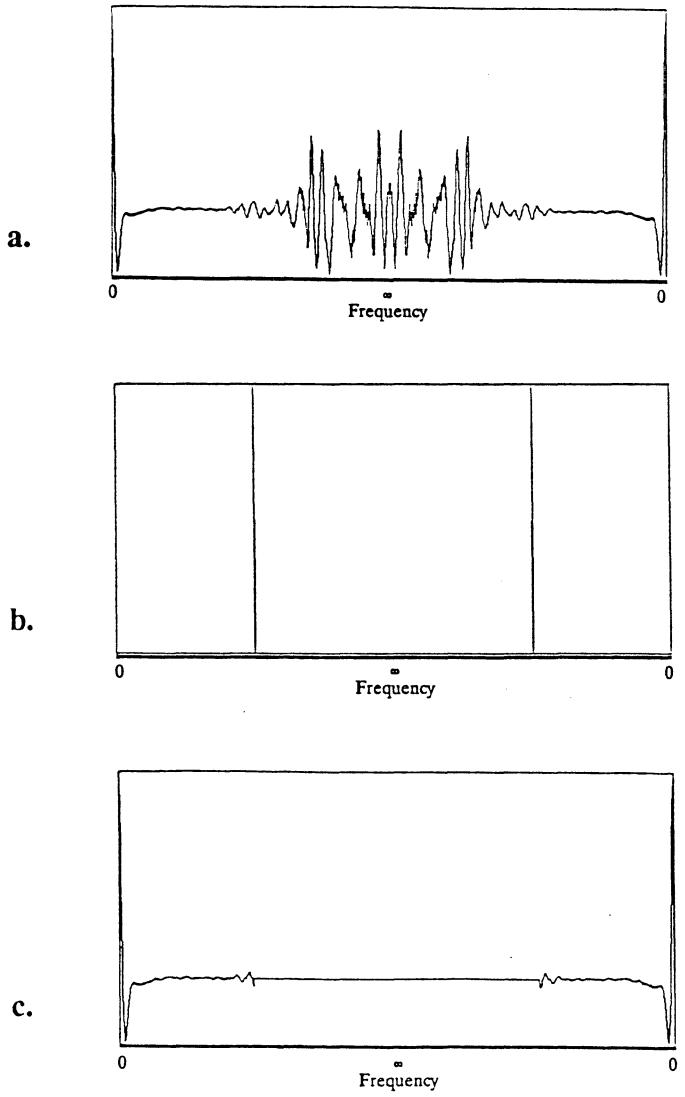

Fig. 13. *Figure* **a** *shows the same transform as in Fig. 11c. It is filtered between the frequencies shown in figure* **b** *(the figure shows the Fourier transform of a sine function with a period of 4 channels, corresponding to 80 ps) and the result is shown in figure* **c**.

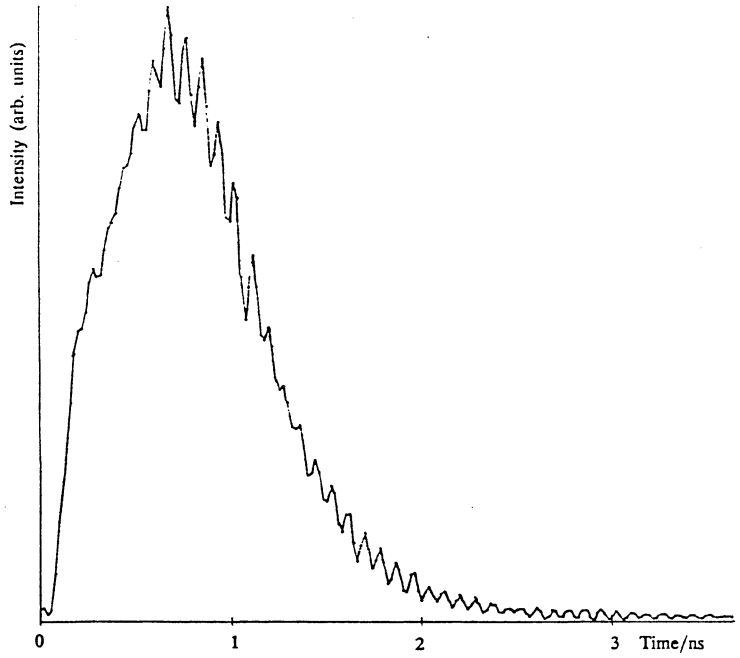

Fig. 14. *The result when the transform in Fig. 13c is inversely transformed.*

4.4 Scanning

First an apparatus function is collected. This is done by sampling scattered light from the laser with the cuvette filled with water. In this way the optical path length will be the same for the apparatus function and the successive samples. The cuvette is then filled with the scattering liquid and a dispersion curve without the metal rod is collected as a "reference". The rod is then placed in the middle of the liquid about 4 mm from the beam-detector line. This corresponds to an x position of 2 mm, i.e. the beam-detector line is located at an x position of 6 mm. A dispersion curve is sampled for 180 s and then the rod is translated perpendicularly towards the beam-detector line and a curve is sampled after every millimetre. The curves are stored in the PC on a hard disk.

The dispersion curves are deconvoluted with the apparatus function. Fig. 15 shows the resulting curves for an x position of 2 mm and 6 mm, i.e. the rod between the laser beam and the detector. It is obvious that there is a larger difference between the two curves at the beginning of the curves than at the end. By concentrating the detection on this early light the contrast can be enhanced.

The sum of the first ten channels of all the collected curves was calculated. As a reference the curve without the rod in the liquid was used. The sum for this curve is 2445. (In fact the sum is 0.2445 but all the curves has been multiplied with 10,000 because the program stores the curves as integers on the disk. The low figure is due to that the curves are automatically normalized to a maximum value of 1.0 when they are deconvoluted). This figure was divided by all the other sums recieved with the metal rod at different x positions. The sums varied between 1401 and 85. The results are plotted as crosses in Fig. 16 as a

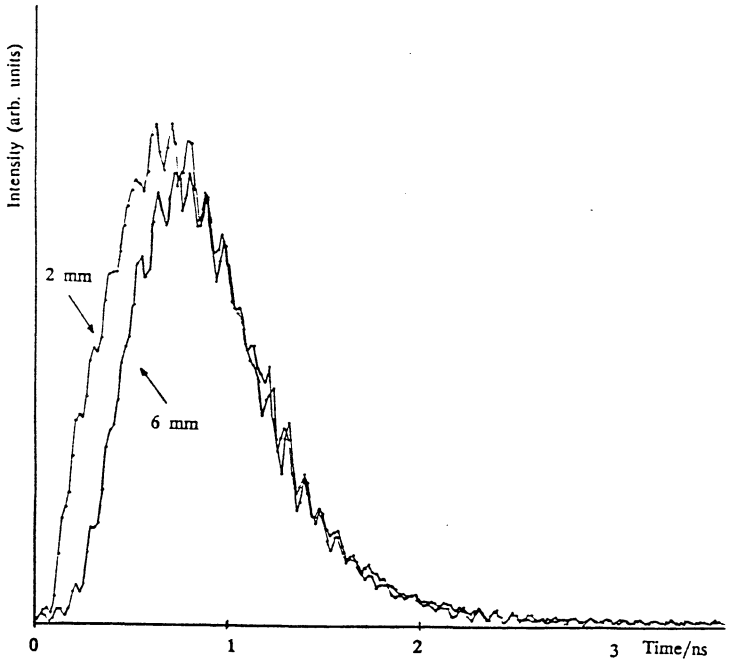

Fig. 15. *The deconvoluted dispersion curves obtained when the metal rod is in x positions 2 mm and 6 mm (6 mm denotes that the rod is between the laser beam and the detector).*

function of the x position. The dashed lines indicate the size and position of the object.

To determine the improvement in the contrast the time-integrated light intensity is also plotted (◇ in Fig. 16). As reference to this curve the count rate, i.e. the light intensity, from the MCP when there is no rod in the liquid is used. It is 2600 cps. This figure is divided by the count rates obtained with the rod scanning across the phantom. These figures vary from 2000 to 1650 cps.

As can be seen from Fig. 16 there is a significant improvement in the contrast when the time-resolved technique is used instead of the light intensity. The maximum ratio between the amount of light detected early without and with the rod between the incident laser beam and the detector is almost 30. The same ratio for the time-integrated light intensity is 1.6.

4.5 Another object

Instead of the metal rod a thin metal plate 8 mm wide was introduced into the phantom. A curve was collected every 2 mm. The sampling time was 180 s at each point and the count rate from the MCP varied between 1500 and 800 cps. The results were evaluated in the same way as for the metal rod (see Fig. 17). In this case the "reference" curve was not a sample without any object in the liquid but the curve sampled at x position 12 mm. There is still a significant demarcation of the object even though the edges of the object are rather blunt. As can be seen in the figure the light intensity curve shows a more pronounced demarcation of the object than in the case of the rod.

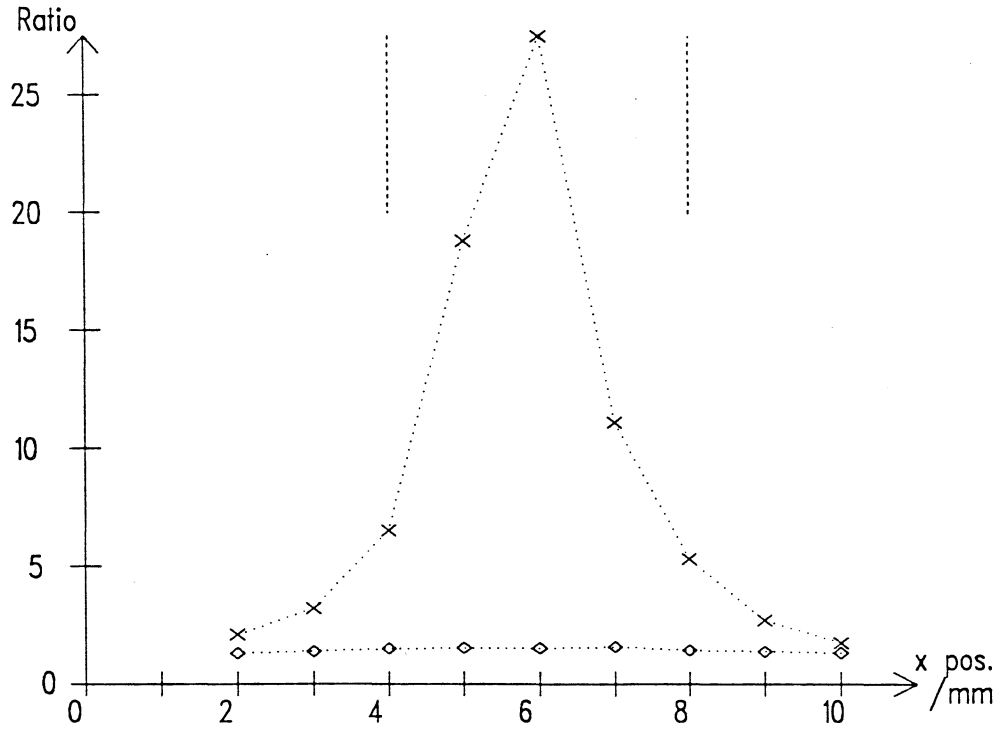

Fig. 16. *The ratio between the sum of the first ten channels of the deconvoluted dispersion curve obtained without any object in the phantom and the same sum with the 4 mm metal rod in different x positions (X). As reference the same ratio for the time-integrated light, i.e. the total light intensity is plotted (◇). The dashed lines indicate the size of the rod. The curve was obtained at a z position of 13 mm.*

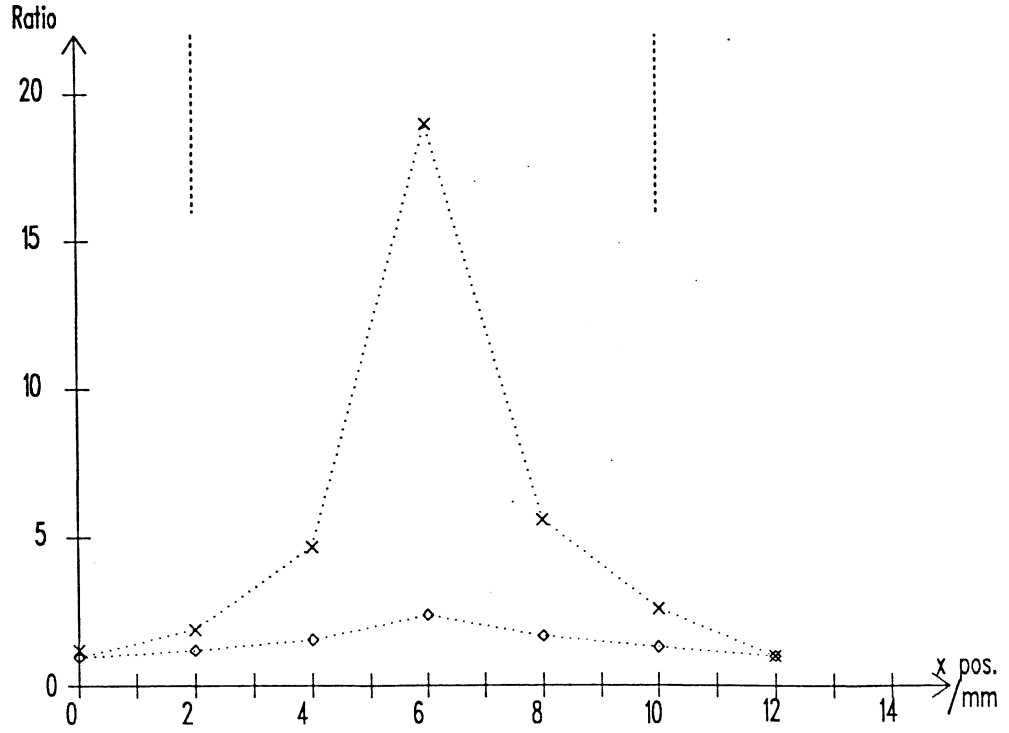

Fig. 17. *The same type of diagram as in Fig. 16 but here the metal rod is replaced by a thin 8 mm wide metal plate (X). As reference sample the dispersion curve obtained at x position 0 mm is used. The time-integrated light intensity is also plotted (◇).*

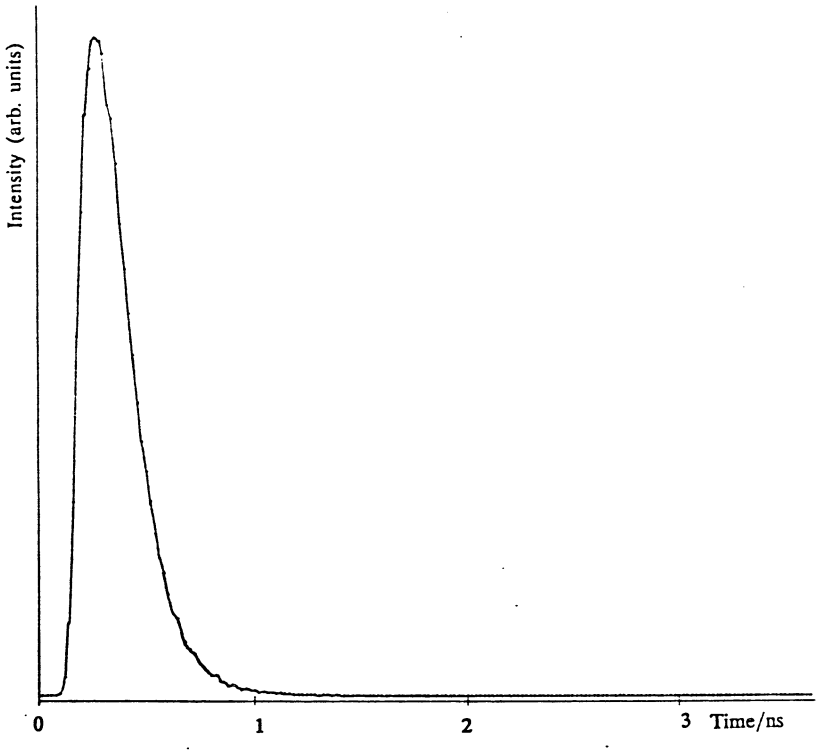

Fig. 18. *The temporal dispersion curve obtained with an 18 mm thick slice of pork as sample.*

4.6 Another sample

Instead of the cuvette with the scattering liquid a piece of pork was used as a sample. This was an ordinary slice of meat bought in a shop and it was 18 mm thick. A dispersion curve is shown in Fig. 18. The dispersion is not as pronounced as it was in the previous sample and this is probably due to higher absorption and the fact that the sample was thinner.

A thin metal plate, 6.5 mm wide, was inserted into the middle of the slice of meat. A scan was performed by moving the slice of meat with the plate in it across the laser-detector line. As the detected light intensity is higher, the MCP count rate was 2950-1150 cps, the sampling time chosen was only 60 s. The curves were deconvoluted and since the dispersion was less here only the first eight channels were summed. The reference curve in this case is the curve sampled in the x position 0 mm. The results are shown in Fig. 19.

There is still a significant difference compared with the light intensity curve. The maximum demarcation is even higher here probably due to the fact that the sample was thinner. There is a fluctuation in this diagram which may be caused by the inhomogeneous structure of the sample.

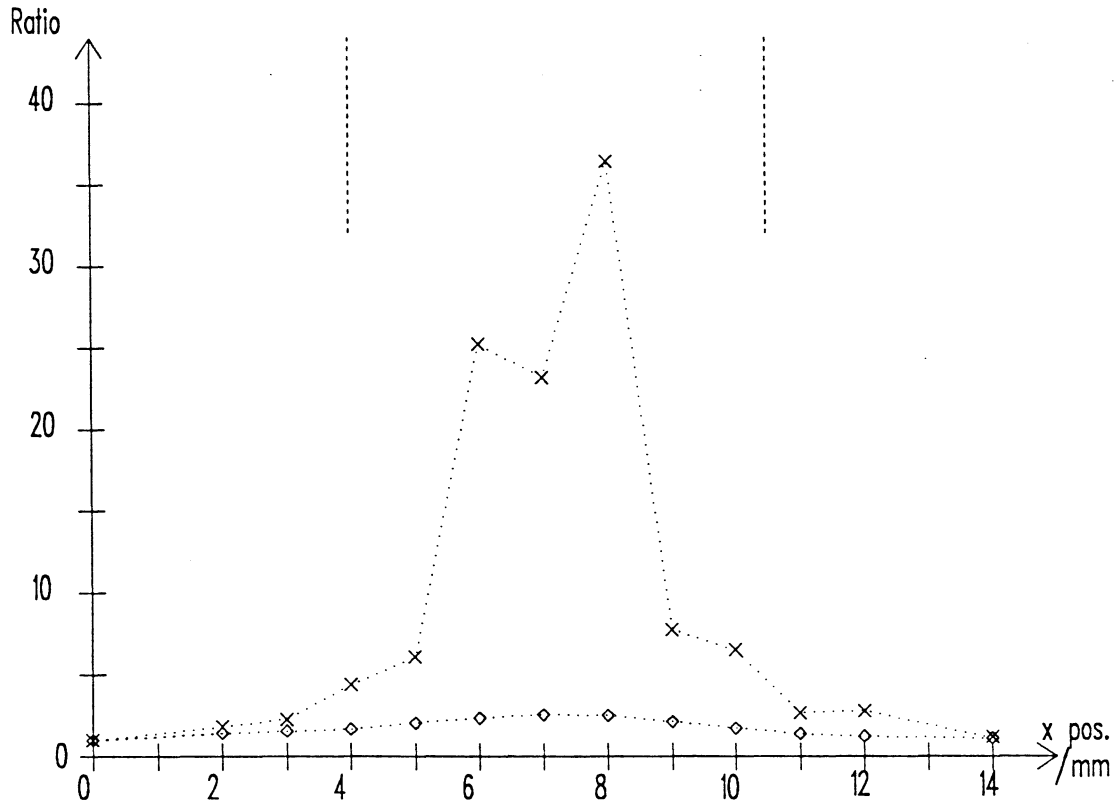

Fig. 19. *The sample for this diagram was the 18 mm thick slice of pork with a 6.5 mm wide metal plate inside it (in the middle of it). The figure shows the ratio between the sum of the first eight channels of the deconvoluted dispersion curve obtained with the sample in x position 0 mm and the same sum with the sample in different x positions (X). As reference the same ratio for the time-integrated light is plotted (◇). The dashed lines indicate the size of the metal plate.*

5 DISCUSSION AND CONCLUSIONS

5.1 The results

The results presented in the figures show a significant improvement in demarcation when the time-resolved technique is was used compared to the curves representing the light intensity scanning. This indicates that the method has a potential. When comparing the results obtained with the rod and the plate as tumour objects it is surprising that the difference is not greater. One would expect the plate to have a better demarcation because it is wider, but perhaps the form of the object is of significant importance. The circumference of the rod is roughly twice the width of the plate. This means that the light absorbing area is of the same order for the two objects and this may be an important factor. It should also be noted that all the results are one dimensional, i.e. no regard has been taken of the shape of the object in the direction perpendicular to the scanning direction.

In evaluating the result, the channels used for gating is of great importance. The number of channels used in this experiment, i.e. ten or eight, were chosen by a trial and error method. The number and the position of the channels were chosen to optimize the result with no theoretical support. Ten channels sounds a lot since this corresponds to a travelled distance of 1.7 times the optical path length of the phantom. To optimize the evaluation a theory for the propagation of the light should be used but that goes beyond the scope of the work presented in this paper.

To improve the results, an experiment was carried out with a polarizer in front of the detector. The incident laser beam is vertically polarized and if a polarizer is placed in front of the detector such that only vertically polarized light is allowed to pass through it may be possible to improve the demarcation. The results showed that the light that exits the phantom is totally unpolarized, i.e. there is as much vertically as horizontally polarized light. This indicates that all the photons used in the time-resolved detection had gone through multiple scattering. The photons that had not been scattered and thus ought still to be vertically polarized are too few to be detected.

5.2 The FFT routine

Since the sampled dispersion curves are Fourier transformed with a computer routine it is interesting to know how well this routine works and whether the curves are distorted in any way. A test shows that if the apparatus function is deconvoluted with itself the result is perfect. This means that the result is a delta function, i.e. one channel is set to one and the rest are zero. This result is obtained when the resulting Fourier transform is not filtered. If the transform is filtered as previously, between channels 250 and 774, the result becomes a function with a FWHM of approx. 2 channels with a slight ripple following the peak.

A test was also carried out with a different filter envelope for the Fourier transform. Instead of cutting off the transform abruptly at channels 250 and 774 an envelope with a slope at these channels was tried. The envelope goes from one at channel 200 in a straight line to

zero at channel 300 and from zero at channel 724 to one at channel 824. When this filter was used in deconvoluting the apparatus function with itself the same peak was obtained but there was a little less ripple after it. When the same filter was used in deconvoluting a sampled dispersion curve and the result is compared with the result obtained with the "abrupt" filter no significant difference could be seen.

5.3 Problems

To get good results it is important that the apparatus function is as narrow as possible. To obtain the 75 ps FWHM apparatus function used in this study quite a lot of trimming had to be carried out on the detector equipment. The part that had to be most carefully adjusted was the constant fraction discriminator. It is important to have as high a trigger level as possible on the input from the PMT to minimize the apparatus function. The cables of the detector equipment were also tried out to optimize the result.

A problem with the detector equipment was that it sometimes suffered from a slight drift. This means that suddenly during a scan a sampled curve could have moved in time compared with the previous curve. The scan then becomes worthless since even a drifting of only one channel makes the different dispersion curves almost impossible to compare. The drifting can be induced by changing the optical path lengths for the light to the trigger diode and the detector or by the detector electronics itself. I strongly suspect the electronics.

Initially, the laser system was not located in the same room as the sample and the detector. The idea was to use an optical fibre to transmit the laser pulses from the laser to the sample. This proved to be a bad idea since the mode dispersion in the fibre distorted and widened the pulse considerably. To circumvent this problem a mono-mode fibre could have been used but then there is the problem of focusing the laser beam onto the very small core of this fibre with a resulting loss of energy. The problem was solved by not using any fibre at all from the laser to the sample. The fibre leading from the detector lens to the PMT is too short to cause any dispersion.

5.4 The future

In order to ascertain whether this technique could be used as a diagnostic method, experiments must be performed on real tissue. In this case the wavelength becomes an important factor. If suitable wavelengths could be chosen, the absorption could be determined at every scanning point, i.e. by sampling with two different wavelengths, one which has a very good absorption in tumour tissue and one which has not, and by comparing these two samples the tumour could be detected without some kind of reference. This assumes that the absorption versus wavelength is well known for tumour tissue and for normal breast tissue.

To improve the technique it could be combined with some kind of tomographic method. By scanning the breast from different angles and using a time-resolved detection technique and then evaluating the result in a tomographic way the contrast could be even more enhanced.

If the method is ever to be clinically usable a different detection technique must be used. To examine a whole breast, hundreds maybe

thousands of points have to be sampled and it is then not acceptable to have a sampling time of several minutes for each point. As a detector a streak-camera could be used. The streak-camera functions like a combination of a photomultiplier tube and a very fast oscilloscope. The incident pulse is directed onto a photocatode, the emitted photo-electrons are multiplied in a microchannel and then the electrons are accelerated towards a phosphor screen. Using deflection plates with a rapidly rising high voltage to guide the electrons the temporal dispersion curve will appear on the screen. In this way a dispersion curve can be obtained with only one incident pulse. The incident light may have to be stronger in order to be able to detect the emitted light with a streak-camera. A suitable laser could be a pulsed and tunable laser of some kind, such as a semi-conductor laser or a Q-switched and mode-locked Nd:YAG/dye laser.

Another method to gate on the early photons could be to use some kind of ultra-fast shutter like a Pockel-cell or a Kerr shutter.

5.5 Conclusions

By using pico-second laser pulses and detecting the emitted light with temporal dispersion from a highly scattering medium the possibility of detecting an absorbing object in the medium can be increased by gating on only the light that arrives early at the detector. In a phantom consisting of a scattering liquid, with scattering qualities not very unlike human tissue and an optical path length of 26 mm, an object of the size 4-8 mm can be detected with a maximum contrast, i.e. the maximum amount of light divided by the minimum amount of light, of 20-30 with this technique compared with a maximum contrast of 1.6-3.2 when all the time-integrated light is detected.

6. ACKNOWLEDGEMENTS

First, I would like to thank my supervisor Stefan Andersson-Engels who has been my guide through this project.

I would also like to thank Jonas Johansson and Jörgen Carlsson for helping me with the equipment, the laser and the detector.

I am also grateful to Anders Persson who has helped me with the computer subroutines I have "borrowed" from him.

And of course I would like to thank Sune Svanberg who came with the idea of this project and made it possible.

7. LIST OF REFERENCES

1. Bartrum Jr. R.J. and Crow H.C., "Transillumination Lightscanning to Diagnose Breast Cancer: A Feasibility Study", American Journal of Radiology, 142:409-414, 1984.

2. Bernro R. and Pettersson I., "Electromagnetic Waves in Tissue", Diploma paper, Lund Institute of Technology, 1987.

3. Ertefai S. and Profio E., "Spectral Transmittance and Contrast in Breast Diaphanography", Medical Physics, 12(4):393-400, 1985.

4. Anderson R.R. and Parrish J.A., "The Optics of Human Skin", The Journal of Investigative Dermatology, 77:13-19, 1981.

5. Eichler J., Knof J. and Lenz H., "Measurements on the Depth of Penetration of Light (0.35-1.0 μm) in Tissue", Rad. and Environm. Biophys., 14:239-242, 1977.

6. Wilson B.C., Jeeves W.P, Lowe D.M. and Adam G., "Light Propagation in Animal Tissue in the Wavelength Range 375-825 Nanometers", In: D.R. Doiron and C.J. Gomer (eds.), *Phorphyrin Localization and Treatment of Tumors* (Alan R. Liss, New York), 115-132, 1984.

7. Carlsen E.N., "Transmission Spectroscopy: An Improvement in Light Scanning", RNM Images, February 1983.

8. Navarro G.A. and Profio A.E., "Contrast in Diaphanography of the Breast", Med. Phys., 15(2):181-187, 1988

9. Ohlsson B., Gundersen J. and Nilsson D-M., "Diaphanography: A Method for Evaluation of the Female Breast", World Journal of Surgery, 4:701-707, 1980.

10. Jackson P.C. et al., "The Development of a System for Transillumination Computed Tomography", The British Journal of Radiology, 60:375-380, 1987.

11. Hallqvist A. and Holm A., "Lasertomografi", Diploma paper, Lund Institute of Technology, 1985.

12. Cope M. and Delpy D.T., "System for Long-Term Measurement of Cerebral Blood and Tissue Oxygenation on Newborn Infants by Near Infra-Red Transillumination", Med. & Biol. Eng. & Comput., 26:289-294, 1988.

13. Chance B. et al., "Comparison of Time-Resolved and -Unresolved Measurements of Deoxyhemoglobin in Brain", Proc. Natl. Acad. Sci. USA, 85:4971-4975, 1988.

14. Delpy D.T., Cope M., van der Zee P., Arridge S., Wray S. and Wyatt J., "Estimation of Optical Pathlength through Tissue from Direct Time of Flight Measurement", Phys. Med. Biol., 33(12):1433-1442, 1988.

15. van der Zee P. and Delpy D.T., "Simulation of the Point Spread Function for Light in Tissue by a Monte Carlo Method", Adv. Exp. Med. Biol., 215:179-92, 1987.

16. Maarek J.M., Jarry G., Crowe J., Bui M.-H. and Laurent D., "Simulation of Laser Tomoscopy in a Heterogeneous Biological Medium", Med. & Biol. Eng. & Comput., 24:407-414, 1986.

17. Wilksch P.A. and Jacka F., "Studies of Light Propagation through Tissue", In: D.R. Doiron and C.J. Gomer (eds.), *Phorphyrin Localization and Treatment of Tumors* (Alan R. Liss, New York), 149-161, 1984.

18. Carlsson J. and Rüter F., "Autocorrelator for Analysis of Picosecond Pulses from a Modelocked Laser", Diploma paper, LRAP-51, Lund Institute of Technology, 1985.

8. APPENDICES

A. THE PICO-SECOND LASER

The pico-second laser used in this study consists of
a) an Ar^+ laser with a mode-locker head
b) a dye laser with a cavity dumper.

Fig. 20 shows the laser system.

The Ar^+ laser

The active medium in the Ar^+ laser is argon gas. The gas is ionized by an electrical current in the discharge tube and the ions are then excited to a higher energy level. In this way a population inversion is induced and the lasing effect can be achieved. Fig. 21 shows the energy levels of the gas. Many different laser wavelengths can be obtained from argon ions but the most important wavelengths are 488 nm and 514 nm. The current in the cavity is concentrated to the centre of the tube by a powerful electrical field and to prevent the argon ions from drifting towards the cathode the gas is forced to circulate by means of a return tube.

Mode-locking

The Ar^+ laser is mode-locked with a mode-locker head. Mode-locking means that the output beam consists of a train of pulses where the time

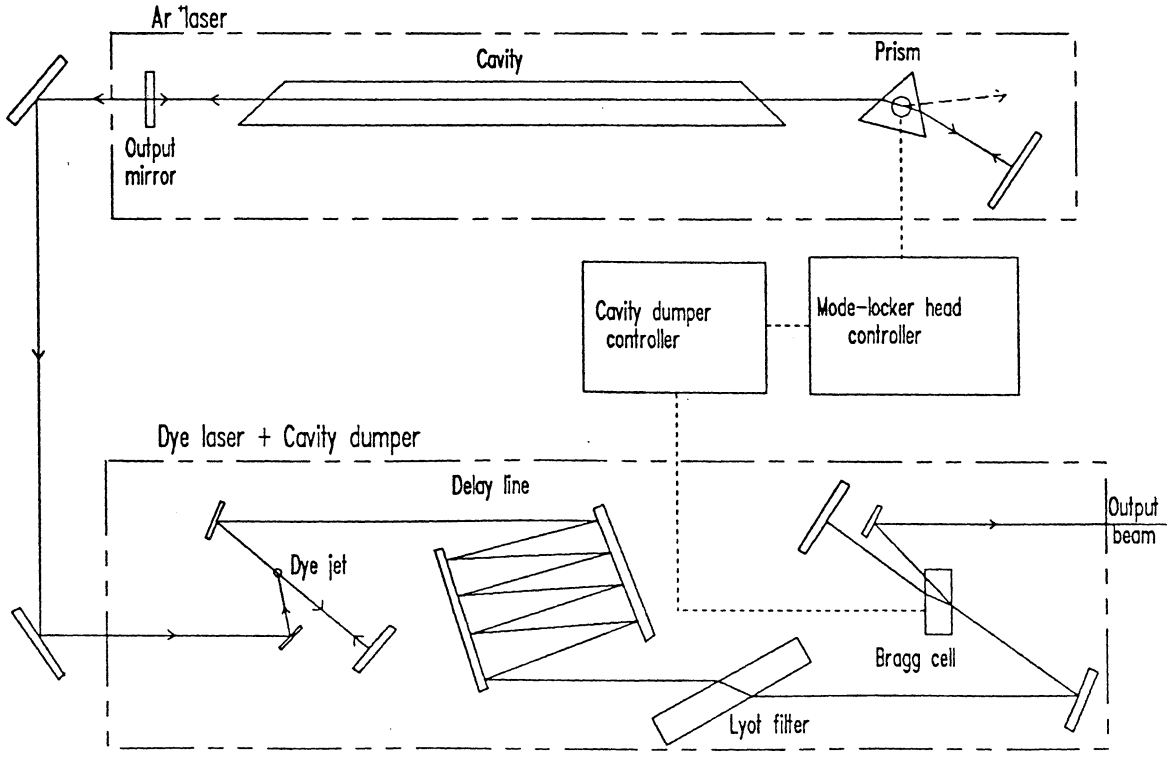

Fig. 20. *The pico-second laser.*

between the pulses corresponds to the round trip time for the laser, i.e. the time it takes for the light to travel back and forth once in the laser. This is achieved by having some sort of gate, which opens and shuts at a frequency corresponding to the round trip time, in front of one of the cavity mirrors and thus only one pulse can be amplified in the cavity.

The mode-locker head consists of a prism to which a piezo-electrical crystal is attached. This system works as an acousto-optic modulator. An RF signal of approx. 37.5 MHz is sent to the crystal from the mode-locker controller. The half period of this frequency corresponds to the round trip time, 13 ns. The crystal induces an acoustic wave of the same frequency in the prism. The length of the prism corresponds to a number of half wavelengths of the wave. Thus a standing wave is created in the prism.

The standing wave gives rise to variations in the pressure and this induces variations in the refractive index. The prism will then work as a grating and the passing light will be diffracted. Twice every period of the wave, though, the standing wave will be "flat" and thus there is no grating effect and the light can pass freely and be reflected back by the cavity mirror. In this way only one pulse is allowed to travel back and forth in the cavity. The prism can be turned to select the desired wavelength.

The dye laser

A dye laser has an organic dye dissolved in a suitable dissolvent (water, methanol, alcohol) as active medium. In this study DCM dissolved in methanol is used. The effect exploited in dye lasers is that the

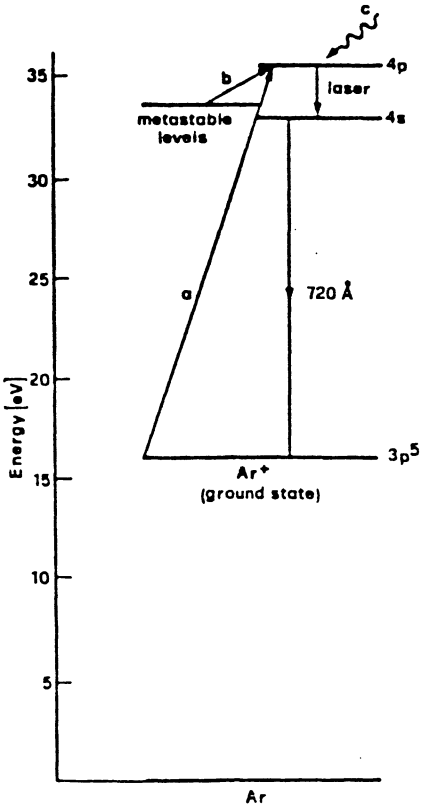

Fig. 21. *The energy levels in the Ar^+ laser.*

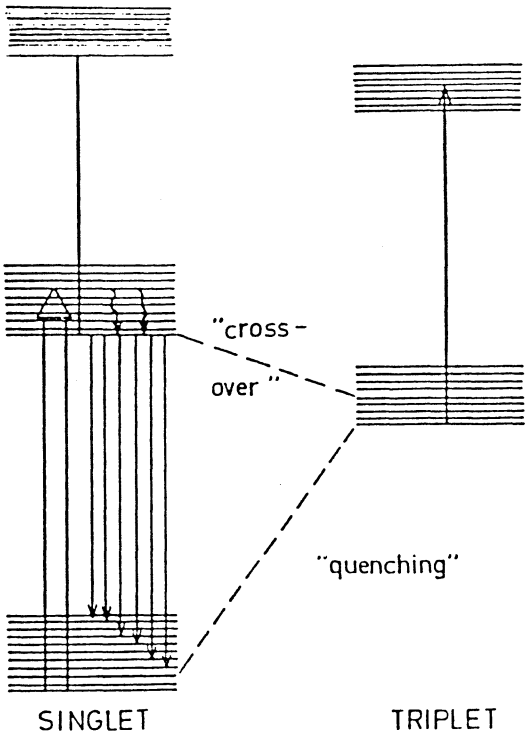

Fig. 22. *The energy bands of a typical dye.*

electronic energy levels for the dye are like broad continuous energy bands. This is due to the many vibrational and rotational levels of the complicated dye molecule. In Fig. 22 the energylevel scheme for a typical dye is illustrated.

Molecules in the lowest singlet level S0 absorb light and are excited to a vibrational-rotational level in the S1 band. The lowest vibrational level of S1 is populated by very fast relaxation through collisions and internal conversion. From here the molecules can deexcite through fluorescence to a vibrational-rotational level in the S0 band. The molecules will then relax quickly to the lowest S0 level. If the dye is pumped, i.e. the molecules are excited, with enough intensity inverted population is achieved between the lowest level of the S1 band and the S0 levels above the lowest level and thus lasing is obtained. Fig. 23 shows the cross section for absorption and fluorescence for the dye Rhodamine 6G.

The excited molecules can be transfered to the triplet level T1 through radiationless intersystem crossings. This is not desirable since these molecules do not participate in the inverted population. The triplet state is also a metastable state so the relaxation to the singlet state takes a considerable time. To avoid having too many molecules in the triplet state in the cavity the dye is circulated with a pump. The triplet molecules then have time to relax in the dye container.

To obtain the laser effect mirrors are introduced to create a cavity. To be able to tune the laser wavelength a double refracting filter, called a Lyot filter, is introduced into the cavity. This filter will suppress all but one selected wavelength.

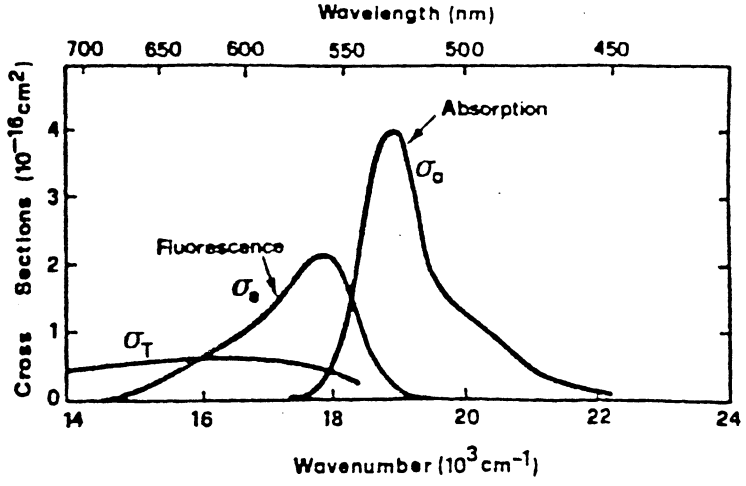

Fig. 23. *The cross section for absorption and fluorescence for Rhodamine 6G.*

The dye laser is mode-locked by synchronous pumping. This means that the cavity length of the pumping laser, in this case the Ar^+ laser, and the cavity length of the dye laser are the same. Thus only one short pulse in the dye laser will be amplified. This pulse will have the same round trip time as the pulses in the pumping laser. To obtain correct cavity length for the dye laser a delay line is introduced. This is a device that reflects the beam back and forth a few times and thus the right length is obtained.

To be able to adjust the pulse repetition frequency and the power of the pulses a cavity dumper is used instead of an ordinary output mirror. The dumper has two highly reflecting mirrors with a Bragg cell in between. The Bragg cell is an acousto-optic modulator in which all the diffracted light is of the first order. It consists of a quartz prism with a piezo-electric crystal attached. If a signal is sent to the crystal, in this case a 380 MHz RF signal, an acoustic wave is created in the prism and thus part of the beam in the cavity will be diffracted out of the cavity. If no signal is sent to the cell no light will come out of the dumper. If the signal to the cell is sent to it in pulses that are shorter than the round trip time and if they are separated by a time which is a multiple of the round trip time the pulse repetition frequency can be chosen.

The repetition frequency is f_0/N where f_0 is the same frequency as that used in the mode-locker head, i.e. approx. 37.5 MHz, and N is an integer which can be chosen between 4 and 259. The smaller the value of N the higher the repetition frequency, but the lower the repetition frequency the higher the peak power in the pulses since they travel back and forth in the cavity more times before they are released and are thus more highly amplified.

The cavity dumper and the mode-locker head on the Ar^+ laser are synchronized.

B. THE AUTOCORRELATOR

When performing time-resolved laser spectroscopy and using a pico-second laser system it is important to be able to measure the length of the laser pulses. To do this an autocorrelator can be used.

Figure 24 shows the construction of the autocorrelator.

The construction of the autocorrelator is based on the Michelson interferometer. The incoming laser pulse is divided perpendicularly by a beam splitter. One of the beams is reflected back by a fixed prism. The other beam is reflected back by a movable prism and then reflected so as to make it parallel to the first beam. The two beams are focused by a lens to a common focus inside a crystal. The crystal is a birefringent crystal, such as KDP, and if the two beams are recombined under the right phase-matching condition a frequency-doubled pulse will be created through second-harmonic generation. The condition that has to be fulfilled is:

$$n2 = n1\cos\phi$$

Here n1 is the refractive index for the incoming pulse, n2 the refractive index for the frequency-doubled pulse and ϕ is half the angle

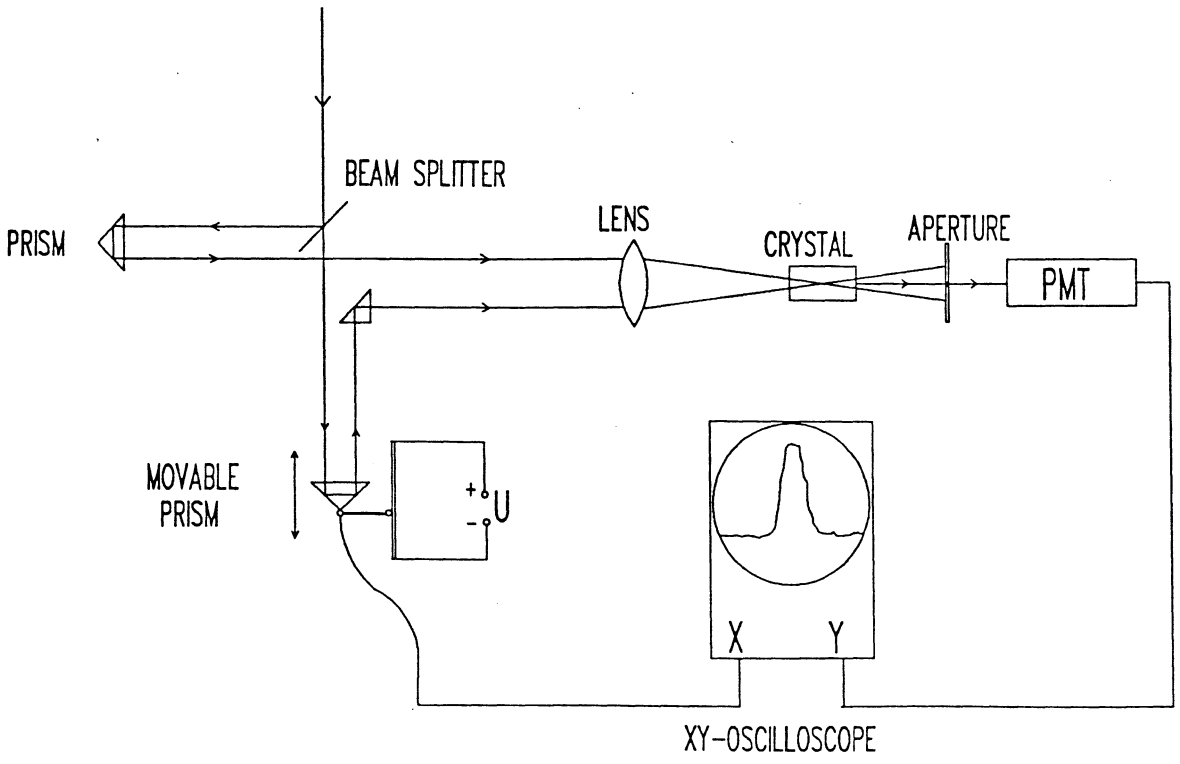

Fig. 24. *The construction of the autocorrelator.*

between the two incoming beams. To fulfil the phase-matching conditions the crystal is rotated along the optical axis which causes n1 to vary between the ordinary index, n_o, and the extraordinary, n_e. The refractive index for the pulse created is thus:

$$(1/n2)^2 = (\cos\theta/n_o)^2 + (\sin\theta/n_e)^2$$

Here θ is the angle between the bisector of the incoming beams and the optical axis of the crystal.

In this way a frequency-doubled pulse will only be created when the difference in the distance travelled between the two beams not exceed the length of the incoming laser pulse. The frequency-doubled signal is detected in a photomultiplier and the signal from this is used as the input for the Y channel on an oscilloscope.

The position of the movable prism is displayed along the X axis on the oscilloscope. This is achieved by connecting a voltage source to a resistance path on which a sliding contact samples the voltage. The contact is located on the same sledge as the movable prism and it is connected to the X channel input on the oscilloscope. By moving the movable prism back and forth, and because the repetition frequency of the pico-second laser is very high (MHz), an image will appear on the oscilloscope. It is not the exact pulse shape that appears but rather the autocorrelation of the pulse. The intensity of the frequency-doubled pulse ($g(\tau)$) for a delay τ is:

$$g(\tau) = C_o \int_{-\infty}^{-\infty} I(t)I(t-\tau)dt$$

Here I(t) is the real pulse-intensity of the incoming pulse and C_o is a constant. If we assume that the measured pulse has a Gaussian shape, i.e. the pulse intensity is proportional to $\exp(-t/T)^2$, then the ratio between the FWHM of the autocorrelated pulse ($\Delta\tau$) and the FWHM of the pulse itself (Δt) is:

$$\Delta\tau/\Delta t = \sqrt{2}$$

C. PROGRAM LISTINGS

In the program EVALUATE the following subroutines are used :

CALCW	Calculates the sine and cosine arrays that the FFT routine uses (listed).
SETAUX	Sets the communication parameters between the MCA and the computer.
TMODE	Clears the screen and sets it in text mode.
TRREAD	Reads a string of data from the MCA.
STOUNF	Stores the data string unformatted on disk.
TRSEND	Sends a data string to the MCA.
REUNF	Reads a string of data from the disk.
GMODE	Clears the screen and sets it in graphic mode.
PVEC	Plots two data strings on the computer screen and marks the "windows", i.e. the channels that are summed.
FFT	Calculates the Fourier transform or the inverse Fourier transform of a string of data (listed).

The program PLOT (which uses the subroutine DATAPLOT) plots a data string on a HP Laserjet printer.

```
      PROGRAM EVALUATE

      IMPLICIT   LOGICAL (A-Z)
      REAL       TWOPI
      INTEGER    N,NOOFWINDOWS,NOOFARRAYS
      PARAMETER  ( N=1024,TWOPI=6.283185308 )
      PARAMETER  ( NOOFWINDOWS=2, NOOFARRAYS=5 )
      REAL       ARRAY(1:NOOFARRAYS,1:N),DUMP
      REAL       SUM(1:NOOFARRAYS,1:NOOFWINDOWS),MAXSIG(1:NOOFARRAYS)
      REAL       MEAN(1:NOOFARRAYS)
      REAL       Y(1:N),DATAARRAY(1:N),DX,DT,SLASK,RP(1:2)
      REAL       WINDIV(1:NOOFARRAYS)
      INTEGER    START(1:NOOFARRAYS),WINL(1:NOOFWINDOWS)
      INTEGER    WINR(1:NOOFWINDOWS),MAXPOS(1:NOOFARRAYS)
      INTEGER    HALF1(1:NOOFARRAYS),HALF2(1:NOOFARRAYS),X,NOW,Z,Q
      INTEGER    I,NCH,NCH2,J,M,BAUDRATE,WORDLENGTH,STOPBITS
      INTEGER    OFF(1:NOOFARRAYS)
      INTEGER*2  ANS,KBDCHK,KBDINC,PAR(1:9)
      COMPLEX    S1(1:NOOFARRAYS,1:2*N),W(1:N),S2(1:2*N)
      CHARACTER  FILENAME*40
      CHARACTER  PARITY*1,SV*1
      LOGICAL    CHECK2,CHECK3,INV,FOUR(1:NOOFARRAYS)
      COMMON     /BLOCK5/ NCH,NCH2,DX
      COMMON     /BLOCK6/ Y,DT

      DO 10 I=1,N
        DATAARRAY(I)=I
        DO 8 X=1,NOOFARRAYS
          ARRAY(X,I)=0.0
          S1(X,I)=0.0
          S1(X,I+N)=0.0
    8   CONTINUE
   10 CONTINUE
      NCH=N
      NCH2=LOG(NCH-0.5)/LOG(2.0)
      NCH2=2**(NCH2+1)

      CALL CALCW(W,NCH2)

      BAUDRATE=9600
      PARITY='E'
      WORDLENGTH=7
      STOPBITS=1
      M=N
      DO 28 X=1,NOOFARRAYS
        MAXPOS(X)=0
        HALF1(X)=0
        HALF2(X)=0
        OFF(X)=0
        START(X)=0
        WINDIV(X)=0.0
        FOUR(X)=.FALSE.
        DO 25 I=1,NOOFWINDOWS
          SUM(X,I)=0.0
          WINL(I)=1
          WINR(I)=1
   25   CONTINUE
   28 CONTINUE
      FOUR(NOOFARRAYS)=.TRUE.
      CALL SETAUX(BAUDRATE,PARITY,WORDLENGTH,STOPBITS)

   30 CALL TMODE

      WRITE(*,100) M,BAUDRATE,PARITY,WORDLENGTH,STOPBITS
  100 FORMAT(/
     fTR20,'Number of channels:',I4,/,/
     fTR1,'F1 : Read from Tracor.',
     fT41,'F2 : Send to Tracor.'/
     fTR1,'F3 : Store on disk, unform. (*.DAT).',
     fT41,'F4 : Read from disk, unform. (*.DAT).'/
     fTR1,'F5 : Set windows.',
     fT41,'F6 : Display.'/
     fTR1,'F7 : Set offset.',
     fT41,'F8 : Set comm. param.',
     f    '(',I4,',',A,',',I1,',',I1,')',/
     fTR1,'F9 : Operation.',
     fT40,'F10 : Fouriertrans.'/
     fTR1,' E : Exit.',/)

      WRITE(*,105) '          Array no. :',(I,I=1,NOOFARRAYS)
  105 FORMAT(A,5I10)
      WRITE(*,107) ('-',I=1,70)
  107 FORMAT('    ',70A)
      WRITE(*,105) '        Maxchannel :',(MAXPOS(X),X=1,NOOFARRAYS)
      WRITE(*,105) '     Left halfw. ch.:',(HALF1(X),X=1,NOOFARRAYS)
      WRITE(*,105) '    Right halfw. ch.:',(HALF2(X),X=1,NOOFARRAYS)
      WRITE(*,105) '            Offset :',(OFF(X),X=1,NOOFARRAYS)
      WRITE(*,110) '         Max value :',(MAXSIG(X),X=1,NOOFARRAYS)
      WRITE(*,110) '    Window1/Window2 :',(WINDIV(X),X=1,NOOFARRAYS)
  110 FORMAT(A,5F10.1)

      DO 115 I=1,NOOFWINDOWS
        WRITE(*,120) I,WINL(I),WINR(I),(SUM(X,I),X=1,NOOFARRAYS)
  120   FORMAT(TR1,'Window',I1,' (',I4,'-',I4,'):',5F10.1)
  115 CONTINUE

   40 ANS=KBDINC()
      IF (ANS.EQ.ICHAR('E').OR.ANS.EQ.ICHAR('e')) THEN
        ANS=11
      ENDIF
      IF (ANS.GE.1059) THEN
        ANS=ANS-1058
      ENDIF
      IF (ANS.LT.1.OR.ANS.GT.12) THEN
        GOTO 40
      ENDIF

      GOTO(1000,2000,3000,4000,6500
     f    ,7000,9000,11000,11500,12000,13000), ANS

*******************************
****** Read from TRACOR ******
*******************************
 1000 CONTINUE
      WRITE(*,1100) 'Read from Tracor.'
 1100 FORMAT(TR20,A)
      CALL TRREAD(DATAARRAY,M)

****** Turn around Y-axis ******
 1500 CONTINUE
      WRITE(*,1600) 'Turn around Y-axis.'
 1600 FORMAT(TR20,A)
      DO 1510 I=1,M/2
        J=M-I+1
        SLASK=DATAARRAY(I)
        DATAARRAY(I)=DATAARRAY(J)
        DATAARRAY(J)=SLASK
 1510 CONTINUE
      WRITE(*,1600) 'Store on disk, unformatted.'
      CALL STOUNF(DATAARRAY,M,FILENAME)
      GOTO 4150

***************************
****** Send to TRACOR ******
***************************
 2000 CONTINUE
      WRITE(*,2100) 'Send to Tracor.'
 2100 FORMAT(TR20,A)
      CALL TRSEND(DATAARRAY,M)
      GOTO 30
```

```
141:
142: ****************************************
143: ****** Store on disk, unformatted ******
144: ****************************************
145: 3000  CONTINUE
146:       WRITE(*,3100) 'Store on disk, unformatted.'
147: 3100  FORMAT(TR1,A)
148: 3110  CONTINUE
149:       WRITE(*,3120) 'Array :'
150: 3120  FORMAT(TR1,A,\)
151:       READ(*,*,ERR=3110) NOW
152:       IF (NOW.LT.1.OR.NOW.GT.NOOFARRAYS) THEN
153:         GOTO 3110
154:       ENDIF
155:       DO 3130 I=1,N
156:         DATAARRAY(I)=ARRAY(NOW,I)
157: 3130  CONTINUE
158:       CALL STOUNF(DATAARRAY,M,FILENAME)
159:       GOTO 30
160:
161: ****************************************
162: ****** Read from disk, unformatted ******
163: ****************************************
164: 4000  CONTINUE
165:       WRITE(*,4100) 'Read from disk, unformatted.'
166: 4100  FORMAT(TR1,A)
167:       CALL REUNF(DATAARRAY,M,FILENAME)
168: 4150  CONTINUE
169:       WRITE(*,4200) 'Array : '
170: 4200  FORMAT(TR1,A,\)
171: 4300  CONTINUE
172:       READ(*,*,ERR=4300) NOW
173:       IF (NOW.LT.1.OR.NOW.GT.NOOFARRAYS) THEN
174:         GOTO 4300
175:       ENDIF
176:       FOUR(NOW)=.FALSE.
177:       DO 4310 I=1,N
178:         ARRAY(NOW,I)=DATAARRAY(I)
179: 4310  CONTINUE
180:
181: ****************************************
182: ******      Calculation           ******
183: ****************************************
184: 5500  CONTINUE
185:       MAXSIG(NOW)=ARRAY(NOW,1)
186:       MEAN(NOW)=0.0
187:       CHECK2=.TRUE.
188:       CHECK3=.TRUE.
189:
190: ***  Find maxpos and -value ***
191:       DO 5510 I=5,N-4
192:         DUMP=0.0
193:         DO 5515 X=I-4,I+4
194:           DUMP=DUMP+ARRAY(NOW,X)
195: 5515    CONTINUE
196:         DUMP=DUMP/9
197:         IF (DUMP.GE.MAXSIG(NOW)) THEN
198:           MAXSIG(NOW)=DUMP
199:           MAXPOS(NOW)=I
200:         ENDIF
201: 5510  CONTINUE
202:
203: ****  Find halfw.  ****
204:       DO 5550 I=3,N-2
205:         DUMP=0.0
206:         DO 5560 J=I-2,I+2
207:           DUMP=DUMP+ARRAY(NOW,J)
208: 5560    CONTINUE
209:         DUMP=DUMP/5
210:         IF (CHECK2) THEN
211:           IF (DUMP.GE.MAXSIG(NOW)/2) THEN
212:             HALF1(NOW)=I
213:             CHECK2=.FALSE.
214:           ENDIF
215:         ENDIF
216:         IF (.NOT.CHECK2.AND.CHECK3) THEN
217:           IF (DUMP.LE.MAXSIG(NOW)/2) THEN
218:             HALF2(NOW)=I
219:             CHECK3=.FALSE.
220:           ENDIF
221:         ENDIF
222: 5550  CONTINUE
223:
224: ***  Go and calculate windows  ***
225:       GOTO 6565
226:
227: ****************************************
228: ****** Set windows  ******************
229: ****************************************
230: 6500  CONTINUE
231:       WRITE(*,6510) NOOFWINDOWS
232: 6510  FORMAT(/,TR1,'Window (1-',I1,'): ',\)
233:       READ(*,*,ERR=6500) I
234:       IF (I.LT.1.OR.I.GT.NOOFWINDOWS) THEN
235:         GOTO 6500
236:       ENDIF
237: 6530  CONTINUE
238:       WRITE(*,6540) N
239: 6540  FORMAT(TR1,'Left limit (1-',I4,') : ',\)
240:       READ(*,*,ERR=6530) WINL(I)
241:       IF (WINL(I).LT.1.OR.WINL(I).GT.N) THEN
242:         GOTO 6530
243:       ENDIF
244: 6550  CONTINUE
245:       WRITE(*,6560) WINL(I),N
246: 6560  FORMAT(TR1,'Right limit (',I4,'-',I4,') : ',\)
247:       READ(*,*,ERR=6550) WINR(I)
248:       IF (WINR(I).LT.WINL(I).OR.WINR(I).GT.N) THEN
249:         GOTO 6550
250:       ENDIF
251:
252: ***   Calculate windows ***
253: 6565  CONTINUE
254:       DO 6590 X=1,NOOFARRAYS
255:         DO 6580 I=1,NOOFWINDOWS
256:           SUM(X,I)=0.0
257:           DO 6570 J=WINL(I),WINR(I)
258:           IF (J+OFF(X).GE.1.AND.J+OFF(X).LE.N) THEN
259:             SUM(X,I)=SUM(X,I)+ARRAY(X,J+OFF(X))
260:           ENDIF
261: 6570      CONTINUE
262: 6580    CONTINUE
263:         IF (SUM(X,2).NE.0.0) THEN
264:           WINDIV(X)=SUM(X,1)/SUM(X,2)
265:         ELSE
266:           WINDIV(X)=0.0
267:         ENDIF
268: 6590  CONTINUE
269:       GOTO 30
270:
271: ********************
272: ****** Display ******
273: ********************
274: 7000  CONTINUE
275:       PAR(1)=0
276:       PAR(2)=0
277:       PAR(3)=719
278:       PAR(4)=347
279:       PAR(5)=1
280:       PAR(6)=0
```

```
      PAR(7)=1
      PAR(8)=0
      PAR(9)=1

      WRITE(*,7005) 'Array 1 (--): '
7005  FORMAT(TR1,A,\)
7006  CONTINUE
      READ(*,*,ERR=7006) I
      IF (I.LT.1.OR.I.GT.NOOFARRAYS) THEN
        GOTO 7006
      ENDIF
      WRITE(*,7005) 'Array 2 (..): '
7008  CONTINUE
      READ(*,*,ERR=7008) J
      IF (J.LT.1.OR.J.GT.N) THEN
        GOTO 7008
      ENDIF

      RP(1)=ARRAY(I,1)
      RP(2)=ARRAY(I,1)
      DO 7010 X=1,M
        RP(1)=MAX(RP(1),ARRAY(I,X),ARRAY(J,X))
        RP(2)=MIN(RP(2),ARRAY(I,X),ARRAY(J,X))
7010  CONTINUE

      IF (ABS(RP(1)-RP(2)).LT.1.0E-2) THEN
        RP(1)=RP(1)+0.5
        RP(2)=RP(2)-0.5
      ENDIF

      SLASK=0.01*(RP(1)-RP(2))
      RP(1)=RP(1)+SLASK
      RP(2)=RP(2)-SLASK

      CALL GMODE
      CALL PVEC(ARRAY,M,PAR,RP,WINL,WINR,NOOFWINDOWS,NOOFARRAYS,I,J,OFF)

7020  ANS=KBDCHK()
      IF (ANS.EQ.0) THEN
        GOTO 7020
      ENDIF
      ANS=KBDINC()

      CALL TMODE
      GOTO 30

************************************
****** Set offset ******************
************************************
9000  CONTINUE
      WRITE(*,9100) 'Array: '
9100  FORMAT(TR1,A,\)
      READ(*,*,ERR=9000) I
      WRITE(*,9200) 'Offset (-50 - +50): '
9200  FORMAT(TR1,A,\)
9150  CONTINUE
      READ(*,*,ERR=9150) OFF(I)
      IF (OFF(I).LT.-50.OR.OFF(I).GT.50) THEN
        GOTO 9150
      ENDIF
      GOTO 6565

****************************************
****** Set communication parameters ******
****************************************
11000 CONTINUE
      WRITE(*,11100) 'Set communication parameters.'
11100 FORMAT(TR20,A)

11010 WRITE(*,11200) 'Baudrate (50..9600):'
11200 FORMAT(' ',A,\)
      READ(*,*,ERR=11010) BAUDRATE
      IF (BAUDRATE.LT.50.OR.BAUDRATE.GT.9600) THEN
        GOTO 11010
      ENDIF

11020 WRITE(*,11200) 'Parity (None, Even, Odd, Mark or Space):'
      READ(*,11300,ERR=11020) SV
11300 FORMAT(A)

      IF     (SV.EQ.'E'.OR.SV.EQ.'e') THEN
        PARITY='E'
      ELSEIF (SV.EQ.'O'.OR.SV.EQ.'o') THEN
        PARITY='O'
      ELSEIF (SV.EQ.'M'.OR.SV.EQ.'m') THEN
        PARITY='M'
      ELSEIF (SV.EQ.'S'.OR.SV.EQ.'s') THEN
        PARITY='S'
      ELSE
        PARITY='N'
      ENDIF

11030 WRITE(*,11200) 'Word length (5,6,7 or 8 bit):'
      READ(*,*,ERR=11030) WORDLENGTH
      IF (WORDLENGTH.LT.5.OR.WORDLENGTH.GT.8) THEN
        GOTO 11030
      ENDIF

11040 WRITE(*,11200) 'Number of stop bits (1 or 2):'
      READ(*,*,ERR=11040) STOPBITS
      IF (STOPBITS.NE.1.AND.STOPBITS.NE.2) THEN
        GOTO 11040
      ENDIF

      CALL SETAUX(BAUDRATE,PARITY,WORDLENGTH,STOPBITS)

      GOTO 30

****************************
****** Operation ***********
****************************
11500 CONTINUE
      WRITE(*,11510) 'First array : '
11510 FORMAT(TR1,A,\)
11520 CONTINUE
      READ(*,*,ERR=11520) I
      IF (I.LT.1.OR.I.GT.NOOFARRAYS) THEN
        GOTO 11520
      ENDIF
      WRITE(*,11510) 'Operation :  F1=(+)  F2=(-)  F3=(*)',
     f'              F4=(/)  F5=(sin)'
11530 ANS=KBDINC()
      IF (ANS.LT.1059.OR.ANS.GT.1063) THEN
        GOTO 11530
      ENDIF
      IF (ANS.EQ.1063) THEN
        WRITE(*,11535) 'Period (chan.) : '
11533   CONTINUE
        READ(*,*,ERR=11533) DUMP
        DO 11534 X=1,N
          ARRAY(I,X)=1*SIN(REAL(X)*TWOPI/DUMP)
11534   CONTINUE
        FOUR(I)=.FALSE.
        NOW=I
        GOTO 5500
      ENDIF
11535 FORMAT(/,TR1,A,\)
      WRITE(*,11535) 'Second array (0=constant) : '
11540 CONTINUE
```

```
      READ(*,*,ERR=11540) J
      IF (J.LT.0.OR.J.GT.NOOFARRAYS) THEN
        GOTO 11540
      ENDIF
      IF (J.EQ.0) THEN
        WRITE(*,11510) 'Constant : '
11545   CONTINUE
        READ(*,*,ERR=11545) DUMP
        IF (DUMP.EQ.0.AND.ANS.EQ.1062) THEN
          GOTO 11545
        ENDIF
        WRITE(*,13100) 'Part of ? (No):'
        READ(*,13200) SV
        IF (SV.EQ.'Y'.OR.SV.EQ.'y') THEN
          WRITE(*,11510) 'Start chan. : '
11547     CONTINUE
          READ(*,*,ERR=11547) Q
          IF (Q.LT.1.OR.Q.GT.N) THEN
            GOTO 11547
          ENDIF
          WRITE(*,11510) 'Stop chan. : '
11548     CONTINUE
          READ(*,*,ERR=11548) Z
          IF (Z.LT.Q.OR.Z.GT.N) THEN
            GOTO 11548
          ENDIF
        ENDIF
      ENDIF
      WRITE(*,11510) 'Result array : '
11550 CONTINUE
      READ(*,*,ERR=11550) NOW
      IF (NOW.LT.1.OR.NOW.GT.NOOFARRAYS) THEN
        GOTO 11550
      ENDIF

      IF (FOUR(I)) THEN
        DO 11560 X=1,N
          IF (J.EQ.0) THEN
            IF (X.GE.Q.AND.X.LE.Z) THEN
              IF (ANS.EQ.1059) THEN
                S1(NOW,X+OFF(NOW))=S1(I,X+OFF(I))+DUMP
              ELSEIF (ANS.EQ.1060) THEN
                S1(NOW,X+OFF(NOW))=S1(I,X+OFF(I))-DUMP
              ELSEIF (ANS.EQ.1061) THEN
                S1(NOW,X+OFF(NOW))=S1(I,X+OFF(I))*DUMP
              ELSE
                S1(NOW,X+OFF(NOW))=S1(I,X+OFF(I))/DUMP
              ENDIF
            ELSE
              S1(NOW,X+OFF(NOW))=S1(I,X+OFF(I))
            ENDIF
          ELSE
            IF (ANS.EQ.1059) THEN
              S1(NOW,X+OFF(NOW))=S1(I,X+OFF(I))+S1(J,X+OFF(J))
            ELSEIF (ANS.EQ.1060) THEN
              S1(NOW,X+OFF(NOW))=S1(I,X+OFF(I))-S1(J,X+OFF(J))
            ELSEIF (ANS.EQ.1061) THEN
              S1(NOW,X+OFF(NOW))=S1(I,X+OFF(I))*S1(J,X+OFF(J))
            ELSE
              S1(NOW,X+OFF(NOW))=S1(I,X+OFF(I))/S1(J,X+OFF(J))
            ENDIF
          ENDIF
11560     CONTINUE
          FOUR(NOW)=FOUR(I)
          DO 11565 X=1,N
            ARRAY(NOW,X)=REAL(S1(NOW,X))
11565     CONTINUE
        ELSE
          DO 11570 X=1,N
            IF (X+OFF(NOW).GE.1.AND.X+OFF(NOW).LE.N.AND.X+OFF(I).GE.1.AND.X+
     f        OFF(I).LE.N) THEN
              IF (J.EQ.0) THEN
                IF (X.GE.Q.AND.X.LE.Z) THEN
                  IF (ANS.EQ.1059) THEN
                    ARRAY(NOW,X+OFF(NOW))=ARRAY(I,X+OFF(I))+DUMP
                  ELSEIF (ANS.EQ.1060) THEN
                    ARRAY(NOW,X+OFF(NOW))=ARRAY(I,X+OFF(I))-DUMP
                  ELSEIF (ANS.EQ.1061) THEN
                    ARRAY(NOW,X+OFF(NOW))=ARRAY(I,X+OFF(I))*DUMP
                  ELSE
                    ARRAY(NOW,X+OFF(NOW))=ARRAY(I,X+OFF(I))/DUMP
                  ENDIF
                ELSE
                  ARRAY(NOW,X+OFF(NOW))=ARRAY(I,X+OFF(I))
                ENDIF
              ELSE
                IF (X+OFF(J).GE.1.AND.X+OFF(J).LE.N) THEN
                  IF (ANS.EQ.1059) THEN
                    ARRAY(NOW,X+OFF(NOW))=ARRAY(I,X+OFF(I))+ARRAY(J,X+OFF(J))
                  ELSEIF (ANS.EQ.1060) THEN
                    ARRAY(NOW,X+OFF(NOW))=ARRAY(I,X+OFF(I))-ARRAY(J,X+OFF(J))
                  ELSEIF (ANS.EQ.1061) THEN
                    ARRAY(NOW,X+OFF(NOW))=ARRAY(I,X+OFF(I))*ARRAY(J,X+OFF(J))
                  ELSE
                    IF (ARRAY(J,X+OFF(J)).LT.1E-3) THEN
                      ARRAY(NOW,X+OFF(NOW))=1.0
                    ELSE
                      ARRAY(NOW,X+OFF(NOW))=ARRAY(I,X+OFF(I))/ARRAY(J,X+OFF(J))
                    ENDIF
                  ENDIF
                ENDIF
              ENDIF
            ENDIF
11570     CONTINUE
        ENDIF

        GOTO 5500

******************
**** Fourier. ****
******************
12000 CONTINUE
      WRITE(*,12010) 'Fouriertr. array : '
12010 FORMAT(1R1,A,\)
12020 CONTINUE
      READ(*,*,ERR=12020) I
      IF (I.LT.1.OR.I.GT.NOOFARRAYS) THEN
        GOTO 12020
      ENDIF
      WRITE(*,12010) 'Result array : '
12050 CONTINUE
      READ(*,*,ERR=12050) NOW
      IF (NOW.LT.1.OR.NOW.GT.NOOFARRAYS) THEN
        GOTO 12050
      ENDIF

      DO 12070 X=1,NCH2
      IF (FOUR(I)) THEN
        S2(X)=S1(I,X)
      ELSE
        IF (X.LE.NCH) THEN
          S2(X)=CMPLX(ARRAY(I,X),0.0)
        ELSE
          S2(X)=CMPLX(0.0,0.0)
        ENDIF
      ENDIF
12070 CONTINUE

      INV=FOUR(I)
      CALL FFT(S2,W,NCH2,INV)
```

```
561:
562:       DO 12080 X=1,NCH2
563:         S1(NOW,X)=S2(X)
564: 12080 CONTINUE
565:
566:       DO 12090 X=1,NCH
567:         ARRAY(NOW,X)=REAL(S2(X))
568: 12090 CONTINUE
569:
570:       FOUR(NOW)=(.NOT.FOUR(I))
571:
572:       GOTO 5500
573:
574: ******************
575: ****** Exit ******
576: ******************
577: 13000 CONTINUE
578:       WRITE(*,13100) 'Exit program? (No):'
579: 13100 FORMAT(' ',A,\)
580:       READ(*,13200) SV
581: 13200 FORMAT(A)
582:       IF (SV.EQ.'Y'.OR.SV.EQ.'y') THEN
583:         STOP
584:       ELSE
585:         GOTO 30
586:       ENDIF
587:
588:       END
```

```
      SUBROUTINE FFT(G,W,N,INV)
*     Anders Persson, 1985

      IMPLICIT   LOGICAL (A-Z)
      COMPLEX    G(0:*),W(0:*),SLASK
      REAL       C
      INTEGER*2  I,J,K,L,M,P,R,S
      INTEGER    N
      LOGICAL    INV

*     *** Butterfly ***
      M=LOG(FLOAT(N))/LOG(2.0)+0.5
      DO 10 K=0,M-1
      DO 10 L=0,N-N/2**K,N/2**K
      DO 10 I=0,N/2**(K+1)-1
        R=L+I
        S=R+N/2**(K+1)
        P=I*2**K
        SLASK=G(R)+G(S)
        IF(INV) THEN
          G(S)=(G(R)-G(S))*CONJG(W(P))
        ELSE
          G(S)=(G(R)-G(S))*W(P)
        ENDIF
        G(R)=SLASK
10    CONTINUE

*     *** Bit reversal ***
      DO 20 I=0,N-1
        K=I
        L=0
        DO 30 J=1,M
          L=L+MOD(K,2)*2**(M-J)
          K=K/2
30      CONTINUE
        IF(L.GT.I) THEN
          SLASK=G(I)
          G(I)=G(L)
          G(L)=SLASK
        ENDIF
20    CONTINUE

*     *** Norm. ***
      C=1.0/FLOAT(N)
      IF(INV) THEN
        DO 40 I=0,N-1
          G(I)=G(I)*C
40      CONTINUE
      ENDIF
      RETURN
      END
```

```
      SUBROUTINE CALCW(W,N)
*     Anders Persson, 1985

      IMPLICIT   LOGICAL (A-Z)
      COMPLEX    W(0:*)
      REAL       FI,TWOPI
      PARAMETER  ( TWOPI=6.283185308 )
      INTEGER    N,I

      FI=-TWOPI/FLOAT(N)
      DO 10 I=0,N/2-1
        W(I)=CEXP(CMPLX(0.0,FI*I))
10    CONTINUE
      RETURN
      END
```

```
      PROGRAM PLOT

      IMPLICIT  LOGICAL (A-Z)
      INTEGER   N
      PARAMETER (N=1024)
      REAL      ARRAY(1:N),MAXI,M,DUMP
      INTEGER   I,LEFT,RIGHT,QD
      CHARACTER FILENAME*12,MSG*12,ANS*1


4000  CONTINUE
      WRITE(*,4100) 'Read from disk, unformatted.'
      CALL REUNF(ARRAY,N,FILENAME)
4100  FORMAT(TR2,A)

      WRITE(*,4110) 'Title : '
4110  FORMAT(TR2,A,\)
4120  CONTINUE
      READ(*,4130,ERR=4120) MSG
4130  FORMAT(A)

      DUMP=ARRAY(1)
      DO 4135 I=1,N
        DUMP=MAX(DUMP,ARRAY(I))
4135  CONTINUE
      WRITE(*,4150) 'Max. value (',DUMP,') :'
4140  CONTINUE
4150  FORMAT(TR2,A,F9.1,A,\)
      READ(*,*,ERR=4140) MAXI

4155  CONTINUE
      WRITE(*,4110) 'Left limit : '
      READ(*,*,ERR=4155) LEFT
      IF (LEFT.LT.1.OR.LEFT.GT.N) THEN
        GOTO 4155
      ENDIF

4160  CONTINUE
      WRITE(*,4110) 'Right limit : '
      READ(*,*,ERR=4160) RIGHT
      IF (RIGHT.LT.LEFT.OR.RIGHT.GT.N) THEN
        GOTO 4160
      ENDIF


      WRITE(*,4100) 'HPstart.'
      CALL HPSTART('L')
      WRITE(*,4100) 'Dataplot.'
      WRITE(*,*) N,MAXI,LEFT,RIGHT
      CALL DATAPLOT(ARRAY,N,MAXI,MSG,LEFT,RIGHT)
      WRITE(*,4100) 'HPeject.'
      CALL HPEJECT

      WRITE(*,4200) 'New parameters (N/*) ? :'
      READ(*,4300) ANS
      IF (ANS.NE.'N') THEN
        GOTO 4135
      ENDIF

      WRITE(*,4200) 'Again (N/*) ? :'
4200  FORMAT(TR2,A,\)
      READ(*,4300) ANS
4300  FORMAT(A)
      IF (ANS.NE.'N') THEN
        GOTO 4000
      ENDIF

      END
```



```
      SUBROUTINE DATAPLOT(ARRAY,N,MAX,MSG,LEFT,RIGHT)

      IMPLICIT  LOGICAL(A-Z)
      INTEGER   I,N,LEFT,RIGHT,NUM
      REAL      ARRAY(1:N),DX,DY,XP,YP
      REAL      MAX,YMAX,YMIN,XMAX,XMIN
      LOGICAL   LANDSCAPE
      CHARACTER MSG*12
      INTEGER*2 XPOS,YPOS,COLOUR,RASTER(0:44,0:1119)
      COMMON    /RGRP/ XPOS,YPOS,LANDSCAPE,COLOUR,RASTER

      XMIN=0
      YMIN=0
      XMAX=719
      YMAX=1119
      IF (LANDSCAPE) THEN
        XMAX=1119
        YMAX=719
      ENDIF
      NUM=RIGHT-LEFT
      DX=REAL(XMAX/NUM)
      DY=REAL((YMAX-10)/MAX)

      XP=NINT(1*DX)
      YP=NINT(ARRAY(LEFT)*DY)+10
      IF (XP.GE.XMIN.AND.XP.LE.XMAX.AND.YP.GE.YMIN.AND.YP.LE.YMAX) THEN
        CALL HPMOVE(XP,YP)
      ENDIF
      DO 100 I=LEFT+1,RIGHT
        XP=NINT((I-LEFT)*DX)
        YP=NINT(ARRAY(I)*DY)+10
        IF(XP.GE.XMIN.AND.XP.LE.XMAX.AND.YP.GE.YMIN.AND.YP.LE.YMAX)THEN
          CALL HPMARK(XP,YP)
        ENDIF
100   CONTINUE

      XP=NINT(0.9*XMAX)
      YP=NINT(0.9*YMAX)
      DO 110 I=1,12
        IF (MSG(1:I).EQ.' ') THEN
          GOTO 120
        ENDIF
110   CONTINUE
120   CONTINUE
      CALL HPPRINT(XP,YP,I,MSG)

      DO 130 I=LEFT,RIGHT,50
        XP=NINT((I-LEFT)*DX)
        YP=YMIN
        IF(XP.GE.XMIN.AND.XP.LE.XMAX.AND.YP.GE.YMIN.AND.YP.LE.YMAX)THEN
          CALL HPMOVE(XP,YP)
        ENDIF
        YP=YMIN+9
        CALL HPDRAW(XP,YP)
130   CONTINUE

      XP=XMIN
      YP=YMAX
      CALL HPMOVE(XP,YP)
      YP=YMIN+4
      CALL HPDRAW(XP,YP)
      XP=XMAX
      CALL HPDRAW(XP,YP)

      RETURN
      END
```